SARS-CoV-2 Cell Entry Factors ACE2 and TMPRSS2 are Expressed in the Pancreas but are Not Enriched in Islet Endocrine Cells

Katie C. Coate[1,*], Jeeyeon Cha[1,*], Shristi Shrestha[1], Wenliang Wang[2], Luciana Mateus Gonçalves[3], Joana Almaça[3], Meghan E. Kapp[4], Maria Fasolino[2], Ashleigh Morgan[2], Chunhua Dai[1], Diane C. Saunders[1], Rita Bottino[5,6], Radhika Aramandla[1], Regina Jenkins[1], Roland Stein[7], Klaus H. Kaestner[2], Golnaz Vahedi[2], HPAP consortium[8], Marcela Brissova[1], Alvin C. Powers[1,7,9,10]

[1]Division of Diabetes, Endocrinology and Metabolism, Department of Medicine, Vanderbilt University Medical Center, Nashville, TN, 37232

[2]Department of Genetics and Institute for Diabetes, Obesity, and Metabolism, University of Pennsylvania Perelman School of Medicine, Philadelphia, PA, 19104

[3]Division of Endocrinology, Diabetes and Metabolism, Department of Medicine, University of Miami Miller School of Medicine, Miami, FL, 33136

[4]Department of Pathology, Microbiology and Immunology, Vanderbilt University Medical Center, Nashville, TN, 37232

[5]Institute of Cellular Therapeutics, Allegheny Health Network, Pittsburgh, PA, 15212

[6]Imagine Pharma, Devon, PA, 19333

[7]Department of Molecular Physiology and Biophysics, Vanderbilt University School of Medicine, Nashville, TN, 37232

[8]The Human Pancreas Analysis Program (RRID:SCR_016202)

[9]VA Tennessee Valley Healthcare System, Nashville, TN, 37212

[10]Lead Contact

[*]Co-first authors

Running Title: ACE2 and TMPRSS2 are Not Enriched in Pancreatic β cells

27 Correspondence: al.powers@vumc.org; marcela.brissova@vumc.org

28 Alvin C. Powers or Marcela Brissova, Vanderbilt University Medical Center, 2215 Garland Ave,

29 Nashville, TN 37232-0475

Summary/Abstract

Reports of new-onset diabetes and diabetic ketoacidosis in individuals with COVID-19 have led to the hypothesis that SARS-CoV-2, the virus that causes COVID-19, is directly cytotoxic to pancreatic islet β cells. This would require binding and entry of SARS-CoV-2 into host β cells via cell surface co-expression of ACE2 and TMPRSS2, the putative receptor and effector protease, respectively. To define ACE2 and TMPRSS2 expression in the human pancreas, we examined six transcriptional datasets from primary human islet cells and assessed protein expression by immunofluorescence in pancreata from donors with and without diabetes. *ACE2* and *TMPRSS2* transcripts were low or undetectable in pancreatic islet endocrine cells as determined by bulk or single cell RNA sequencing, and neither protein was detected in α or β cells from these donors. Instead, ACE2 protein was expressed in the islet and exocrine tissue microvasculature and also found in a subset of pancreatic ducts, whereas TMPRSS2 protein was restricted to ductal cells. The absence of significant ACE2 and TMPRSS2 co-expression in islet endocrine cells reduces the likelihood that SARS-CoV-2 directly infects pancreatic islet β cells through these cell entry proteins.

46 **Introduction**

47 In coronavirus disease of 2019 (COVID-19), elevated plasma glucose levels with or without pre-
48 existing diabetes and BMI have been identified as independent risk factors of morbidity and
49 mortality with severe acute respiratory syndrome-associated coronavirus-2 (SARS-CoV-2)
50 infection (Barron et al., 2020; Cariou et al., 2020; Holman et al., 2020; Riddle et al., 2020;
51 Wang, 2020; Zhou et al., 2020). Isolated cases of new-onset diabetes and diabetic emergencies
52 such as ketoacidosis and hyperosmolar hyperglycemia have been reported with COVID-19
53 (Chee et al., 2020; Goldman et al., 2020; Hollstein et al., 2020; Kim et al., 2020; Li et al., 2020a;
54 Rafique and Ahmed, 2020; Unsworth et al., 2020), leading to the hypothesis that SARS-CoV-2
55 has a diabetogenic effect mediated by direct cytotoxicity to pancreatic islet β cells (Koch, 2020).

56 *In vitro* studies have shown that SARS-CoV-2 entry into human host cells requires
57 binding to the cell surface receptor angiotensin converting enzyme 2 (ACE2) as well as
58 proteolytic cleavage of the viral spike (S) protein by transmembrane serine protease 2
59 (TMPRSS2) (Hoffmann et al., 2020; Lan et al., 2020; Shang et al., 2020; Wiersinga et al., 2020).
60 In 2010, Yang and colleagues (Yang et al., 2010) examined autopsy samples from a single
61 deceased patient infected by SARS-CoV-1, which uses similar machinery for binding and
62 cellular entry, and reported expression of ACE2 in pancreatic islet cells. Though the identity of
63 these islet cells was not assessed, the authors suggested that binding of ACE2 by SARS-CoV-1
64 damages islets and causes acute diabetes, which could be reversed after viral recovery (Yang
65 et al., 2010). There have been occasional reports of other viral infections eliciting a diabetogenic
66 effect (reviewed in (Filippi and von Herrath, 2008)). More recently, Yang and colleagues
67 reported that β-like cells derived from human pluripotent stem cells (hPSCs) as well as β cells of
68 primary human islets express ACE2, raising the possibility of direct infection and cytotoxicity of
69 β cells by SARS-CoV-2 (Yang et al., 2020). Importantly, neither of these prior studies (Yang et
70 al., 2010; Yang et al., 2020) characterized the expression and localization of TMPRSS2, an

71 obligate co-factor for SARS-CoV-2 cellular entry. Thus, a more detailed analysis of both ACE2
72 and TMPRSS2 expression and localization in human pancreatic tissue from normal donors and
73 those with diabetes is urgently needed. The purpose of this study was to test the hypothesis that
74 native pancreatic islet β cells possess the cellular machinery that could render them direct
75 targets of SARS-CoV-2. Importantly, we found that ACE2 and TMPRSS2 protein are not
76 detectable in human islet endocrine cells from normal donors or those with diabetes, making a
77 direct diabetogenic effect of SARS-CoV-2 via ACE2 and TMPRSS2 unlikely.
78

Results and Discussion

ACE2 and *TMPRSS2* mRNA expression is minimal in human α or β cells.

We first evaluated mRNA expression of *ACE2* and *TMPRSS2* from two existing bulk RNA-sequencing (RNA-seq) datasets (Arda et al., 2016; Blodgett et al., 2015) where human islet α and β cells were enriched by fluorescence activated cell sorting and compared their expression to that of key islet-enriched genes, some of which are normally expressed at relatively low levels in islet cells (e.g., transcription factors). Median expression level of *ACE2* and *TMPRSS*2 mRNA was much less than transcripts of such key islet-enriched genes in human α and β cells (~84% and 92% lower than α and β cell-enriched transcripts, respectively) (**Figure 1A;** n=7-8 adult donors per study). In addition, analysis of four single-cell (sc) RNA-seq datasets of human pancreatic cells (Baron et al., 2016; Camunas-Soler et al., 2020; Kaestner et al., 2019; Segerstolpe et al., 2016) revealed that, in aggregate, less than 1.5% of β cells expressed *ACE2* or *TMPRSS2*, and each transcript was minimally expressed or undetectable in all other endocrine cell subsets (**Figure 1B, S4J** and **Table S1**). We note that this includes analysis of the robust Human Pancreas Analysis Program (HPAP) dataset that includes more than 25,000 cells from 11 normal donors (Kaestner et al., 2019), findings of which are confirmed in the analyses of three previously reported, but smaller, datasets (**Figure 1B** and **S4J**). Furthermore, given that *ACE2* and *TMPRSS2* co-expression is required for canonical SARS-CoV-2 host cell entry (Hoffmann et al., 2020), we also evaluated this occurrence but found that no β cells co-expressed *ACE2* and *TMPRSS2* in any of these four datasets (**Table S1**).

As for non-endocrine cells, the HPAP dataset (Kaestner et al., 2019) revealed that a small subset (< 5%) of endothelial and stellate cells (which include pericytes) expressed moderate to high levels of *ACE2*, whereas only ~1-3% of either population expressed *ACE2* in the datasets by Baron and colleagues (Baron et al., 2016) and Segerstolpe and colleagues (Segerstolpe et al., 2016) (**Figure 1B**). This difference most likely stems from the number of

104 cells analyzed in that the HPAP dataset contains ~2.5- and 20-fold more cells than that of Baron
105 et al. (Baron et al., 2016) or Segerstolpe et al. (Segerstolpe et al., 2016), respectively. In
106 addition, pooled analysis of these datasets (Baron et al., 2016; Camunas-Soler et al., 2020;
107 Kaestner et al., 2019) showed that less than 1% of acinar or ductal cells expressed *ACE2*,
108 whereas ~35% of both cell types expressed *TMPRSS2*. In the dataset by Segerstolpe and
109 colleagues (Segerstolpe et al., 2016), *ACE2* was expressed in ~20% of acinar and ductal cells,
110 whereas *TMPRSS2* was expressed in greater than 75% of both populations (**Figure 1B**).
111 Evaluation of *ACE2* and *TMPRSS2* co-expression in non-endocrine cells revealed that on
112 average, less than 1% of acinar, ductal, endothelial and stellate cells co-expressed both
113 transcripts in these datasets (Baron et al., 2016; Camunas-Soler et al., 2020; Kaestner et al.,
114 2019). In the Segerstolpe et al. dataset (Segerstolpe et al., 2016), ~5% of acinar cells and 15%
115 of ductal cells co-expressed *ACE2* and *TMPRSS2*, but this difference could represent
116 unintended cell selection bias as this study analyzed the fewest number of cells.
117 Altogether, these gene expression findings reduce the likelihood that SARS-CoV-2 can
118 bind and enter human β cells via the canonical pathway involving ACE2 and TMPRSS2.
119 However, they do not exclude the possibility of viral entry via non-canonical pathways involving
120 other suggested effector proteases of SARS-CoV-2, such as Cathepsin L (*CTSL*), ADAM
121 metallopeptidase domain 17 (*ADAM17*), *FURIN* and *TMPRSS4* (Breidenbach et al., 2020;
122 Schreiber et al., 2020; Seyedpour et al., 2020; Zang et al., 2020). We evaluated the expression
123 of these transcripts across all four scRNA-seq datasets and found that with the exception of
124 *TMPRSS4*, each is ubiquitously expressed to varying degrees in all cell types (**Figure 1B,**
125 **Table S1**). In aggregate, however, less than 1% of β cells co-expressed *ACE2* with *CTSL*,
126 *ADAM17*, *FURIN* or *TMPRSS4* (**Table S1**). An outstanding question is whether expression of
127 these transcripts in even 1% of β cells is sufficient to confer permissiveness to SARS-CoV-2
128 infection *in vivo*. Furthermore, heparan sulfate in the extracellular glycocalyx (Clausen et al.,

129 2020) and motile cilia (present on islet endocrine cells) (Lee et al., 2020) were mechanisms
130 proposed to assist ACE2-mediated viral entry. Future studies addressing these possibilities in β
131 cells are urgently needed. Notwithstanding, *CTSL*, *ADAM17*, *FURIN* and *TMPRSS4* were more
132 highly expressed in exocrine, endothelial and stellate cells, as was ACE2 (**Figure 1B**). These
133 gene expression patterns raise the possibility that infection of certain pancreatic cell types by
134 SARS-CoV-2 indirectly impacts β cell function.

135 Obesity is a key metabolic risk factor associated with mortality with COVID-19. A recent
136 report noted increased correlation of *TMPRSS2*, but not *ACE2*, expression with BMI (Taneera et
137 al., 2020). We evaluated the expression of *ACE2*, *TMPRSS2* and *ADAM17* in β cells from 11
138 donors according to their BMI in our largest sc-RNAseq dataset (Kaestner et al., 2019). We did
139 not observe changes in the expression of *ACE2* or *TMPRSS2* expression with increasing BMI
140 but observed a trend towards higher *ADAM17* expression (**Figure S1**). However, this dataset
141 included only one patient with an obese BMI. Studies with a larger number of donor islets are
142 needed to address the role of obesity and other pancreas-resident SARS-CoV-2 effector
143 molecules on β cell function in the context of COVID-19.
144

145 **ACE2 and TMPRSS2 protein are not detected in adult or juvenile human islet α or β cells.**
146 Recently, Yang and colleagues (Yang et al., 2020) reported that ACE2 protein was present in α
147 and β cells from primary human islets and in β-like cells derived from hPSCs. To investigate
148 ACE2 expression, we immunostained cryosections of intact isolated human islets using the
149 same ACE2 antibody as used by Yang and colleagues (Yang et al., 2020) (antibody validation
150 studies in **Figure S2**). In accordance with the transcriptomic data reported above, ACE2 was
151 not detected in insulin-positive β cells or glucagon-positive α cells in our samples; instead,
152 ACE2 signal was prominent in surrounding cells such as those of the microvasculature (**Figure**
153 **1C, top panels**).

154 Since hPSC-derived β-like cells differentiated *in vitro* are considered "juvenile-like" and not
155 functionally mature β cells (Nair et al., 2019), one possibility is that ACE2 is expressed in less
156 differentiated cells, or in the cultured, immortalized β cells (EndoCβH1) studied by Fignani et al.
157 (preprint: Fignani, 2020). We investigated such a possibility by staining for ACE2 in pancreatic
158 sections from juvenile human donors (age range 5 days to 5 years) using the same ACE2
159 antibody as used by Yang et al. (Yang et al., 2020). However, ACE2 was not detected in these
160 juvenile β or α cells (**Figure 1C, bottom panels**), making this explanation less likely.
161 To further characterize ACE2 and TMPRSS2 protein expression in the native pancreas, we
162 next analyzed human pancreatic tissue sections from normal donors (ND, n=14; age range 18-
163 59 years) and those with type 2 diabetes (T2D, n=12; age range 42-66 years) or type 1 diabetes
164 (T1D, n=11; age range 13-63 years) for these proteins on the same sections. ACE2 protein did
165 not co-localize with markers of α or β cells but was detected within the distinct islet areas
166 indicative of microvascular structures in all ND individuals (**Figures 2A-C", 2D-F"** and **S3A-D**)
167 as well as those with T2D (**Figures 2G-I", 2J-L"** and **S3I-L**) or T1D (**Figures 2M-O", 2P-R"** and
168 **S3O-R**). We noted similar findings with three additional ACE2-directed antibodies, including the
169 same antibodies and dilutions reported by Yang et al. (Yang et al., 2020) and by Fignani et al.
170 (preprint: Fignani, 2020), and one antibody validated by the Human Protein Atlas (HPA) (Hikmet
171 et al., 2020) (**Figure S2**). Three of these antibodies detect epitopes corresponding to the
172 extracellular domain of ACE2 (AF933; MAB933; HPA000288), while one detects an epitope in
173 the C-terminal domain (ab15348). Staining patterns were similar across all antibodies (**Figure**
174 **S2**). Furthermore, ACE2 antibody specificity (ab15348) was confirmed via peptide competition
175 with the commercially available immunizing peptide (**Figure S2F-I**).
176 TMPRSS2 protein was not detected within islets in ND (**Figures 2A-C", 2D-F"** and **S3E-H**),
177 T2D (**Figures 2G-I"**, **2J-L"** and **S3M-N**), or T1D donors (**Figures 2M-O", 2P-R"** and **S3S-V**).
178 The TMPRSS2-positive structures in exocrine tissue resembled intercalated and larger ducts as

179 indicated by the typical organization of their nuclei (**Figures 2C”**, **2F”, 2I”, 2L”, 2O” and 2R”**).
180 We did not detect differences in the signal intensity or spatial distribution of ACE2 or TMPRSS2
181 between ND and T2D tissue (**Figures 2** and **S3**) but labeling for both proteins appeared to be
182 reduced in T1D pancreatic sections (**Figure 2M-R” and S3O-V**). Altogether, these observations
183 indicate that the cell surface proteins required for canonical SARS-CoV-2 host cell entry were
184 not detected on islet endocrine cells from normal or diabetic donors.

185 Recent in silico analyses by Vankadari et al. (Vankadari and Wilce, 2020) and Li et al. (Li et
186 al., 2020b) suggested that human dipeptidyl peptidase 4 (DPP4) may interact with SARS-CoV-2
187 and facilitate its entry into host cells. Therefore, we examined the distribution of DPP4 in human
188 pancreas and found that it localized to α cells, but not β cells, of ND, T2D and T1D islets
189 (**Figure S4A-I**). This finding is consistent with our analysis of four scRNA-seq datasets showing
190 *DPP4*-enriched α cells (**Figures 1B and S4J**). Given that we did not detect TMPRSS2 within
191 islets, these data suggest that DPP4 is an unlikely mediator of β cell entry by SARS-CoV-2
192 (Drucker, 2020).

193 The discrepancy between our findings and those of recent studies identifying ACE2 and
194 TMPRSS2 in human β cells (Yang et al., 2010) (Yang et al., 2020) (preprint: Fignani, 2020) is
195 likely explained by important differences in experimental approaches and contexts. Yang et al.
196 (Yang et al., 2010) showed ACE2 staining in a single donor islet but did not identify its cellular
197 identity with endocrine markers. Furthermore, the ACE2 antibody used in their study was not
198 reported, which precluded replication of their finding. Fignani et al. (preprint: Fignani, 2020)
199 identified ACE2 protein in presumed islet endocrine cells from seven non-diabetic donors;
200 however, ACE2 was primarily seen in subcellular compartments rather than the expected cell
201 surface location. Colocalization of ACE2 with insulin granules in this study raises the possibility
202 of a staining artifact. Furthermore, Yang et al. (Yang et al., 2020) examined ACE2 expression in
203 isolated dispersed human islet cells, whereas our study examined ACE2 in isolated intact islets

204 and in human islets of native pancreata. It is possible that dispersion of pancreatic cells may
205 have altered the expression of ACE2 in this context (van den Brink et al., 2017). Likewise,
206 sources of variability in immunostaining techniques can stem from differences in tissue fixation
207 procedures, antigen retrieval methods, antibodies used and their dilutions. Notwithstanding, the
208 remarkable concordance of our findings with those from a recent independent effort in native
209 pancreas (Kusmartseva, et al) suggest that differences in experimental conditions may explain
210 the discordance with other studies.
211
212 **ACE2 is localized to islet and exocrine tissue capillaries.**
213 The non-endocrine cell staining pattern of ACE2 in islets prompted us to examine whether
214 ACE2 was expressed in the microvasculature, as described in other organs (Hamming et al.,
215 2004). Indeed, staining of adult and juvenile human pancreatic tissue sections with CD31, an
216 endothelial cell marker, revealed that ACE2 labeling was localized to the perivascular
217 compartment of islet capillaries (**Figures 3A-D', I-L'** and **S5A-H'**). In addition, exocrine tissue
218 capillaries, similar to those in islets, showed perivascular ACE2 labeling (**Figures 3E-H'** and
219 **S5I-P'**). As ACE2-positive cells were scarce in T1D pancreatic tissues (**Figures 2M, 2O'-O",**
220 **2P, 2R'-R",** and **S3O-R**), the presence of ACE2 labeling in the perivascular compartment was
221 relatively rare in both islet (**Figure S5E-H'**) and exocrine (**Figure S5M-P'**) T1D tissues. The
222 structure and close relationship between ACE2-positive perivascular cells and CD31-positive
223 endothelial cells in islet and exocrine tissue capillaries raised the possibility that ACE2-positive
224 cells were in fact pericytes enveloping capillary endothelial cells of the vascular tube (Almaca et
225 al., 2018). In addition, we observed ACE2-positive cytoplasmic processes extending along
226 CD31-positive endothelial cells colocalized with the extracellular matrix marker collagen-IV
227 within the vascular basement membrane (**Figures 3D'**, **3H'**, **S5D'**, **S5H'**, **S5L' and S5P'**), a
228 pattern that is consistent with pericyte morphology (Almaca et al., 2018).

229 To address this observation more directly, we visualized ACE2 expression in relationship to
230 known pericyte markers and found that ACE2 was enriched in pericyte populations expressing
231 PDGFRβ (**Figure 4A-D**). Indeed, colocalization analysis revealed that ~60% of ACE2-positive
232 cells were PDGFRβ-positive (**Figure 4H-I**). Since PDGFRβ labels pericytes and perivascular
233 fibroblasts (Almaca et al., 2020), we also stained tissues with a more specific pericyte marker,
234 NG2, and found that ~30% of ACE2-positive cells were NG2-positive (**Figure 4E-G', 4H-I**).
235 These data agree with our scRNA-seq analysis of the HPAP dataset which identified a subset of
236 pericytes, marked by *PDGFRB*, that express moderate levels of *ACE2* (**Figure 1B**). In addition,
237 our findings support recent reports of pericyte-specific vascular expression of ACE2 in brain and
238 heart tissue (Chen et al., 2020; He, 2020). Emerging evidence from both pre-clinical models of
239 SARS-CoV-2 infection (Aid, 2020) and patients with COVID-19 indicate that cells of the
240 microvasculature (e.g. endothelial cells and pericytes) are requisite contributors to the initiation
241 and propagation of severe disease (Teuwen et al., 2020). Although we found that *TMPRSS2*
242 expression was negligible in endothelial and stellate cells (which includes pericytes) of human
243 islets, *CTSL*, *ADAM17*, *FURIN* and *ACE2* were moderately to highly expressed in these
244 populations (**Figure 1B**), raising the intriguing possibility of direct infection of cells in the islet
245 microvasculature by SARS-CoV-2. Such an occurrence could trigger β cell dysfunction and the
246 metabolic sequelae of COVID-19. Future studies addressing this possibility in human islets and
247 pancreatic tissue are urgently needed.
248
249 **Both ACE2 and TMPRSS2 protein are present in pancreatic ducts but rarely are co-**
250 **expressed.**
251 Our work indicated that TMPRSS2 protein was localized to the apical surface of intercalated
252 and larger ducts in ND (**Figures 2B, 2C", 2E, 2F"** and **S3E-H**), T2D (**Figures 2H, 2I", 2K, 2L"**
253 and **S3M-N**), and T1D pancreatic tissues (**Figures 2N, 2O", 2Q, 2R"** and **S3S-V**). To further

254 define ductal expression of TMPRSS2 and determine whether ACE2 was expressed beyond
255 exocrine tissue capillaries, we visualized expression of these two proteins in relationship to
256 cytokeratin-19 protein (KRT19), a ductal cell marker. TMPRSS2, but not ACE2, was expressed
257 by KRT19-positive cells on the apical surface of intercalated and larger ducts throughout the
258 exocrine compartment (**Figure 5A-D'**). Rarely, both ACE2 and TMPRSS2 were found on the
259 apical surface of ductal epithelial cells but were spatially distinct (**Figure 5E-H'**). These findings
260 agree with our scRNA-seq analysis in which *TMPRSS2* was more highly expressed in ductal
261 cells than *ACE2*, but cells positive for both *ACE2* and *TMPRSS2* were rare. In addition,
262 although *TMPRSS2* mRNA was detected in acinar cells by scRNA-seq (**Figure 1B**), TMPRSS2
263 protein was undetectable by immunofluorescence analysis (**Figure 5**), indicating that studies of
264 mRNA and protein may be discordant.

265 Because rare cells in the exocrine compartment co-express ACE2 and TMPRSS2, it is
266 possible that SARS-CoV-2 could infect those cells, induce pancreatitis, and consequently
267 impact islet function. While recent case reports of patients with COVID-19 have noted mild
268 elevations of amylase and lipase or frank pancreatitis (Karimzadeh et al., 2020; Meireles et al.,
269 2020; Rabice et al., 2020; Wang et al., 2020), the vast majority of patients with COVID-19 have
270 neither elevated pancreatic enzymes nor frank pancreatitis (Ashok et al., 2020; Bonney et al.,
271 2020; Bruno et al., 2020). To investigate this possibility, we analyzed the histology of pancreatic
272 tissue obtained at autopsy from seven COVID-19 positive patients, three of whom had diabetes.
273 We did not find signs of pancreatitis, interstitial edema, inflammatory infiltrate, hemorrhage or
274 necrosis (**Figure 5I**). It is important that exocrine inflammation and ACE2/TMPRSS2 expression
275 be analyzed in a larger number of COVID-19 autopsy samples, particularly in those with new-
276 onset diabetes. Such studies will be challenging since the pancreas rapidly undergoes autolysis
277 upon death.

278 In summary, recent reviews, commentaries, and clinical guidelines (Apicella et al., 2020;
279 Bornstein et al., 2020; Goldman et al., 2020; Gupta et al., 2020; Heaney et al., 2020) have

280 highlighted an attractive hypothesis of direct cytotoxicity by SARS-CoV-2 to β cells. Here, we
281 addressed the fundamental question of whether canonical SARS CoV-2 cell entry machinery is
282 present in β cells of human pancreatic tissue. By examining pancreatic ACE2 and TMPRSS2
283 expression in normal donors and in those with diabetes, we found that, **1)** β cells do not
284 coexpress *ACE2* and *TMPRSS2* transcripts by scRNA-seq analysis and neither protein is
285 detectable in α or β cells by immunofluorescence; **2)** ACE2 is primarily expressed in the islet
286 and exocrine tissue capillaries, including pericytes, as well as a subset of ductal cells; **3)**
287 TMPRSS2 is primarily expressed in ductal cells; **4)** ACE2 and TMPRSS2 are infrequently co-
288 expressed in pancreatic ducts; **5)** ACE2 and TMPRSS2 protein expression and distribution
289 appear similar in ND and T2D pancreata but studies on additional pancreata are needed to
290 definitively answer this question; and **6)** Alternative pathways facilitating SARS-CoV-2 viral
291 infection in β cells cannot be excluded. These findings align considerably with independent
292 observations from Kusmartseva and colleagues (Kusmartseva, 2020) and do not support the
293 hypothesis that SARS-CoV-2 binds and infects islet β cells via a canonical pathway mediated by
294 ACE2 and TMPRSS2, eliciting a diabetogenic effect. As outlined below in the "Limitations of the
295 Study" section, additional studies are needed to investigate whether direct SARS-CoV-2
296 infection of β cells occurs or is detrimental to β cell health or function by other mechanisms.
297 However, based on current data, it appears that the interaction of diabetes and SARS-CoV-2 is
298 mediated by systemic inflammation and/or metabolic changes in other organs such as liver,
299 muscle or adipose tissue.
300

301 **Limitations of the Study**

302 We did not directly measure SARS-CoV-2 binding or entry into human β cells but instead
303 assessed expression of canonical co-receptors, ACE2 and TMPRSS2, in the human pancreas.
304 While studies culturing SARS-CoV-2 and human islets *in vitro* will be of considerable interest,

305 such experiments may be challenging to interpret as the islet isolation process itself may impact
306 ACE2 or TMPRSS2 expression or susceptibility to viral infection. In addition, infection of islet
307 cells within an intact, isolated islet with a variety of viruses has proven difficult as is selection of
308 an appropriate ratio of viral particles and islet cells reflective of the *in vivo* environment.
309 Furthermore, it is not clear if infection of an isolated islet accurately models the physiology of a
310 vascularized, innervated islet within the context of the pancreas.

311 While the preponderance of research suggests that ACE2 and TMPRSS2 are the primary
312 means for SARS-CoV-2 entry into host cells, knowledge about additional pathways and/or
313 mechanisms of SARS-CoV-2 cell entry and infection is rapidly evolving. We sought, but did not
314 find evidence, suggesting that other proposed pathways (namely *DPP4*, *CTSL*, *ADAM17*,
315 *FURIN* or *TMPRSS4*) are involved in β cell entry.

316 We did not assess the presence of SARS-CoV-2, its proteins, or RNA in the pancreas from
317 COVID-19-infected individuals. It is possible that SARS-CoV-2 could infect pancreatic exocrine
318 cells, ductal cells, endothelial cells, or microvasculature, leading to pancreatic inflammation that
319 negatively impacts β cell health or function. We did not find evidence of inflammation in the
320 pancreas of seven COVID-19-infected patients (three of whom had diabetes). Future efforts are
321 needed to collect a large number of pancreata from COVID-19-infected individuals with and
322 without diabetes (long-standing and recent-onset) to search for presence of SARS-CoV-2 or
323 inflammation (islet or exocrine). Since the pancreas undergoes rapid autolysis after death, care
324 must be taken to collect the pancreas very soon after death for this analysis.

325

326 **Acknowledgements**

327 We are especially thankful to organ donors and their families. This research was supported by
328 funding provided by the National Institute of Diabetes and Digestive and Kidney Diseases, the
329 Human Islet Research Network (HIRN; RRID:SCR_014393; https://hirnetwork.org; DK112232,

330 DK123716, U01DK123594, DK104211, DK108120), and by DK106755, DK117147, DK117147-
331 01A1S1, DK111757, DK112217, DK20593, and the Functional Genomics Core of DK19525.
332 This manuscript used data acquired from and available at the Human Pancreas Analysis
333 Program (HPAP-RRID:SCR_016202) Database (https://hpap.pmacs.upenn.edu), a HIRN
334 consortium. This work was also supported by grants from the Doris Duke Charitable Foundation
335 (DDCF 4043516256), Human Islet Research Network New Investigator Pilot Award (UC4
336 DK104162), JDRF, The Leona M. and Harry B. Helmsley Charitable Trust, and the Department
337 of Veterans Affairs (BX000666). Human pancreatic islets were provided by the NIDDK-funded
338 Integrated Islet Distribution Program at the City of Hope (NIH Grant # 2UC4 DK098085 RRID:
339 SCR_014387; http://iidp.coh.org). Human kidney sections were provided by Dr. Agnes B. Fogo
340 at Vanderbilt University Medical Center. We thank Amber M. Bradley for technical assistance.
341
342 **Author Contributions:** K.C. J.C., M.B., and A.C.P. designed the experiments. K.C., J.C., M.B.,
343 and A.C.P. wrote the manuscript. K.C., J.C., S.S., W.W., L.G. J.A., M.E.K., M.F., A.M., C.D.,
344 D.S., R.B., R.J., R.W.S., K.L.H., G.V., M.B., and A.C.P. performed experiments or analyzed the
345 data. All authors reviewed and edited the final manuscript. As the lead contact, A.C.P. is
346 responsible for: 1) communication with the journal and co-authors; 2) addressing requests for
347 reagents and resources; and 3) overseeing decisions and disputes related to the manuscript.
348
349 **Declaration of Interests:** The authors declare no conflicts of interests.
350

351 **Figure 1. *ACE2* and *TMPRSS2* Expression is Minimal in Isolated Human Islet α and**
352 **β Cells.** (**A**) Relative expression of *ACE2* and *TMPRSS2* compared with select α (white bars)
353 and β (green bars) cell type-enriched genes in sorted human islet α and β cells from previously
354 published bulk RNA-seq datasets, reported as transcript per million mapped reads (TPM; n=7;
355 (Blodgett et al., 2015)) or reads per kilobase of transcript per million mapped reads (RPKM;
356 n=8; (Arda et al., 2016)). Mean expression values are presented as $\log_2$ (TPM+1) or $\log_2$
357 (RPKM+1) to account for negative values. Dotted line highlights *ACE2* and *TMPRSS2*
358 expression. (**B**) Dot plots of *ACE2*, *TMPRSS2*, *CTSL*, *ADAM17*, *FURIN*, *TMPRSS4*, and *DPP4*
359 expression compared with cell type-enriched genes from three single cell (sc) RNA-seq
360 datasets (Baron et al., 2016; Kaestner et al., 2019; Segerstolpe et al., 2016). Dot size indicates
361 percentage of cells in a given population expressing the gene; dot color represents scaled
362 average expression. Dotted lines highlight expression of the putative SARS-CoV-2 entry
363 machinery. Percentages of β cells expressing and co-expressing these genes are available in
364 Table S1. (**C**) Representative images showing an isolated islet from an adult human donor (top
365 panels) and a pancreatic section from a juvenile human donor (bottom panels) stained for ACE2
366 (red; antibody ab15348), insulin (INS; green), glucagon (GCG; white), and DAPI (blue). Dotted
367 yellow line denotes islet area. Scale bar is 50 μm. Human pancreatic donor information is
368 available in Table S2 (1C, donors I1-I3, J1-J5). See also Figures S1, S2, and S4.
369
370 **Figure 2. ACE2 and TMPRSS2 Protein are Not Detected in Human Islet α or β Cells in**
371 **Adult Pancreas.** Immunostaining does not detect SARS-CoV-2 cell entry markers ACE2 (**A**, **D**,
372 **G**, **J**, **M**, **P**; antibody AF933; in red) or TMPRSS2 (**B**, **E**, **H**, **K**, **N**, **Q;** in green), in islet β cells
373 (INS, blue; **C-C'**, **I-I'**, **O-O'**) or islet α cells (GCG; blue; **F-F'**, **L-L'**, **R-R'**) in native pancreatic
374 sections from adult donors without diabetes (**A-F"**) or from donors with type 2 (**G-L"**) or type 1
375 (**M-R"**) diabetes. Dotted yellow lines denote islets. Islet (i) and exocrine (e) inset areas are

376 marked by yellow boxes in MERGE column with DAPI counterstain. Pancreatic ducts, identified
377 structurally by rosette pattern of DAPI-labeled nuclei (white), are shown within dotted yellow
378 lines in exocrine INSET column. Scale bars are 50 μm (**A-R**) and 25 μm (Insets, **C'-R"**). Human
379 pancreatic donor information is available in Table S2 (**A-F"**, donor N9; **G-L"**, donor 2H; **M-R"**,
380 donor 1C). See also Figures S2, S3, and S4.
381
382 **Figure 3. ACE2 Protein is Localized to Islet and Exocrine Capillaries in Adult and Juvenile**
383 **Human Pancreata.** Representative images of endothelial cells (CD31, white) and ACE2-
384 positive perivascular cells (red; antibody ab15348) in the adult islet (**A-D**') and exocrine (**E-H'**)
385 microvasculature, as well as in juvenile human islet (**I-L'**) microvasculature. Yellow arrowheads
386 point to CD31-positive endothelial cells, while magenta arrowheads point to perivascular ACE2-
387 positive cells. ACE2-positive perivascular cells abut the extracellular matrix marker collagen-IV
388 within the vascular basement membrane (collagen-IV [COL4], green; **D, D', H, H'**). Inset areas
389 (**A'-L'**) are marked by yellow boxes in **A-L**. In juvenile human pancreas (**I-L'**), ACE2 is not
390 detected in islet endocrine cells expressing insulin and glucagon (ENDO, green); DAPI (blue).
391 Scale bars are 50 μm (**A-L**) and 10 μm (Insets, **A'-L'**). Human pancreatic donor information is
392 available in Table S2 (**A-H'**, donor N2; **I-L'**: donor J4). See also Figure S5.
393
394 **Figure 4. ACE2 Protein is Expressed by Islet Pericytes.** (**A-C**) Maximum intensity projection
395 of representative confocal images labelled for platelet-derived growth factor receptor β-positive
396 cells (PDGFRβ, red) and ACE2 (green) in perivascular cells within a normal adult human islet;
397 nuclear DAPI (blue). (**D**) Image of the same islet shown in A-C with insulin labeling (blue).
398 Region within the yellow box in **D** is displayed in **A-C**. (**E-G**) Maximal intensity projection of
399 pericyte labeling with an antibody against the pericyte marker neuron-glial antigen 2 (**E**, NG2,
400 red) colocalized with ACE2 labeling (**F**, green) and nuclear DAPI (blue) in a normal adult human

401 islet (**E-F**). (**G**) Image of the same islet shown in E-F with insulin labeling (blue). Regions within
402 yellow boxes containing pericytes in **G** denote inset areas (**G'**) and represent a subset of islet
403 ACE2-expressing pericytes. (**H**) Colocalization of ACE2 with NG2- or PDGFRβ-positive cells. (**I**)
404 Quantification of ACE2-positive cells expressing pericyte markers NG2 and PDGFRβ. Shown
405 are average values obtained for 3 confocal planes per islet for a minimum of 5 islets per each
406 donor of a given age. Scale bars are 20 μm (**A-C**), 40 μm (**D-G**), and 10 μm (**G'**). Human
407 pancreatic donor information is available in Table S2 (**A-I,** donors HP1754, HP2041, HP2091).
408 See also Figure S5.
409
410 **Figure 5. Analysis of ACE2 and TMPRSS2 Protein Expression in Pancreatic Ducts and**
411 **Pancreatic Histology.** (**A-D'**) TMPRSS2 (green), but not ACE2 (red; antibody R&D AF933), is
412 expressed by KRT19-positive cells (blue) on the apical surface of intercalated and larger ducts
413 throughout the exocrine compartment. DAPI (white). Yellow arrowheads point to TMPRSS2 on
414 the apical surface of ductal cells (KRT19-positive). Magenta arrowheads point to ACE2-positive
415 non-ductal cells. (**E-H'**) Rarely, both TMPRSS2 (green) and ACE2 (red; antibody R&D AF933)
416 were expressed on the apical surface of ductal epithelial cells (KRT19, blue), but appeared to
417 be spatially distinct. Yellow and white arrowheads point to spatially distinct TMPRSS2 and
418 ACE2 labeling, respectively, localized to the apical surface of larger ducts (KRT19-positive
419 cells). Inset areas (**A'-H'**) are marked by yellow boxes in **A-H**. Scale bars are 50 μm (**A-H**) and
420 10 μm (**A'-H'**). (**I**), Representative H&E image of human pancreas upon autopsy after COVID-19
421 disease. None of the seven donor samples evaluated showed signs of pancreatitis as
422 determined by the histological absence of interstitial edema and inflammatory infiltrate,
423 hemorrhage or necrosis. BV, blood vessel; D, duct. Scale bar in green is 100 μm. Human
424 pancreatic donor information is available in Table S2 (**A-D'**, donor N8; **E-H'**, donor N9; **I**,
425 COVID-19 donor 1). See also Figure S3.

426 **STAR METHODS**

427

428 **Resource Availability**

429

430 ***Lead contact.*** Further information and requests for resources and reagents should be directed
431 to and will be fulfilled by the Lead Contact, Alvin C. Powers (al.powers@vumc.org).

432

433 ***Materials Availability.*** This study did not generate new unique reagents.

434

435 ***Data and Code Availability.*** All data generated or analyzed during this study are included in
436 this published article or in the data repositories listed in the Key Resources Table.
437 Original/source data for Figure 1A (bulk RNA-seq of FACS sorted human islet α and β cells) is
438 available under NCBI GEO accession numbers GSE67543 (Blodgett et al., 2015) and
439 GSE57973 (Arda et al., 2016). Original/source data for Figure 1B and Figure S4J (single cell
440 RNA-seq of human islets) is available under NCBI GEO accession number GSE84133 (Baron
441 et al., 2016), GSE124742 (Camunas-Soler et al., 2020), and ArrayExpress (EBI) accession
442 number E-MTAB-5061 (Segerstolpe et al., 2016). This manuscript used data acquired from the
443 Human Pancreas Analysis Program (HPAP) Database (https://hpap.pmacs.upenn.edu), a
444 Human Islet Research Network consortium.

445

446 **Experimental Model and Subject Details**

447

448 ***Human Subjects.*** Pancreata and islets from juvenile, adult, T1D and T2D human donors were
449 obtained through partnerships with the International Institute for Advancement of Medicine
450 (IIAM), National Disease Research Interchange (NDRI), Integrated Islet Distribution Program

451 (IIDP), and local organ procurement organizations. Pancreata from normal donors were
452 processed either for islet isolation (Balamurugan et al., 2003) and/or histological analysis as
453 described previously (described below and in Table S2) (Brissova et al., 2018; Dai et al., 2017).
454 Pancreata from COVID-19 decedents after autopsy were obtained from the Translational
455 Pathology Shared Resource (TPSR) at Vanderbilt University Medical Center (Nashville, TN) and
456 and processed for histological analysis as according to standard procedures for clinical
457 diagnostics (VUMC Histology Peloris Processing Protocol). Samples from donors of both sexes
458 were used in our analyses. Donor demographic information is summarized in Table S2. The
459 Vanderbilt University Institutional Review Board does not consider de-identified human
460 pancreatic specimens to be human subjects research.
461
462

463 **METHOD DETAILS**

464

465 **Human Pancreas Procurement and Preparation of Tissue for Histological Analysis.**
466 Pancreata from juvenile, adult, T1D and T2D donors were obtained within 18 hours from cross-
467 clamp and maintained in cold preservation solution on ice until processing, as described
468 previously (Balamurugan et al., 2003; Brissova et al., 2018). Pancreata recovered from seven
469 COVID-19 decedants were obtained from Vanderbilt University Medical Center (Nashville, TN)
470 within 8-27 hours of death. Donor demographic information is summarized in Table S2. Human
471 kidney samples were provided by Dr. Agnes Fogo, Vanderbilt University. The Vanderbilt
472 University Institutional Review Board has declared that studies on de-identified human
473 pancreatic specimens do not quality as human subjects research.

474

475 **Mouse Tissue Preparation for Histological Analysis.** Mice were maintained on standard
476 rodent chow under a 12-hour light/dark cycle. Kidney from adult NOD.*Cg-Prkdc*^{scid}*Il2rg*^{tm1Wjl}/ Sz
477 (NSG) mice ages 12 to 18 weeks (Jackson Laboratory) were isolated. Tissue specimens were
478 processed for cryosections as described previously (Brissova et al., 2018).

479

480 **Immunohistochemical Analysis.** Immunohistochemical analysis was performed on 5-µm
481 cryosections (Figure 1C; Figure 3 and 4; Figure S2:A-I; S3A-D, I-L and O-R; S4 and S5) or
482 formalin-fixed paraffin embedded (FFPE) pancreatic sections (Figure 2 and 5; Figure S2:J-W;
483 S3E-H, M-N and S-V) as indicated and described previously (Brissova et al., 2014; Brissova et
484 al., 2018; Wright et al., 2020). FFPE sections were first deparaffinized in xylene and ethanol
485 followed by heat-induced epitope retrieval in a citrate-based antigen unmasking solution, pH 6.0
486 (see Key Resource Table). Immunofluorescence analysis of isolated islets was performed on 8-
487 µm cryosections of islets embedded in collagen gels as described previously (Brissova et al.,
488 2005; Brissova et al., 2018). Primary antibodies to all antigens and their working dilutions are

489 listed in the Key Resource Table. The antigens were visualized using appropriate secondary
490 antibodies listed in the Key Resource Table. Digital images were acquired with an Olympus
491 FLUOVIEW FV3000 laser scanning confocal microscope (Olympus Corporation).
492
493 **Peptide Competition.** We combined 1µg of anti-ACE2 antibody (ab15348) with or without 10µg
494 of the immunizing human ACE2 peptide (ab15352) in antibody buffer solution (0.1% Triton X-
495 100/1% BSA/1X PBS) and incubated overnight at 4°C with gentle agitation.
496 Immunofluorescence staining of 5-µm serial cryosections from the same donor was performed
497 as described above. One section was incubated with the neutralized antibody buffer while the
498 other section was incubated with the non-neutralized antibody buffer. ACE2 staining patterns
499 were visualized via confocal microscopy as described above.
500
501 **H&E Staining.** FFPE pancreas tissue sections (5-µm sections, n=7 donors) were processed
502 according to standard procedures for clinical diagnostics (Vanderbilt University Medical Center
503 Histology Peloris Processing Protocols). Slides were stained with hematoxylin & eosin and
504 reviewed by a clinical pathologist (M.E.K.) at Vanderbilt University Medical Center.
505
506 **Bulk RNA-seq Data Acquisition.** Transcripts Per Million (TPM) and Reads Per Kilobase Per
507 Million (RPKM) normalized counts were extracted from publicly available RNA-seq datasets
508 (Arda et al., 2016; Blodgett et al., 2015). The sources of the datasets are summarized in the Key
509 Resources Table. GraphPad Prism v8 was used to generate plots in Figure 1A.
510
511 **Single Cell RNA-seq Data Acquisition.** Raw gene count matrices were extracted from existing
512 single cell RNA-seq datasets (Baron et al., 2016; Segerstolpe et al., 2016; Yang et al., 2020)
513 and from the Human Pancreas Analysis Program (HPAP) Database
514 (https://hpap.pmacs.upenn.edu), a Human Islet Research Network consortium. The sources of

515 the datasets are summarized in the Key Resources Table. Gene count matrices were further
516 analyzed using the R package Seurat version 3.1 (Stuart et al., 2019). Gene count
517 measurements were normalized for each cell by library size and log-transformed using a size
518 factor of 10,000 molecules per cell. The data was further scaled to unit variance and zero mean
519 implemented in the "ScaleData" function. Cell types already annotated by the authors in the
520 original study were used and thus, no clustering was performed. Seurat's "DotPlot" function was
521 used to generate plots shown in Figures 1B and S4J to visualize *ACE2* and *TMPRSS*2 scaled
522 expression.
523
524 **QUANTIFICATION AND STATISTICAL ANALYSIS**
525
526 **Statistical analysis.** Bulk RNA-seq data are expressed as mean ± standard error of mean
527 (Figures 1A). Sample size (n) is provided as the number of independent donor samples. A p-
528 value less than 0.05 was considered significant. Statistical analysis (unpaired t-test) was
529 performed using GraphPad Prism software. Mander's coefficients were determined to quantify
530 colocalization between pericyte markers (NG2 and PDGFRβ) and ACE2 in confocal images of
531 islets using the ImageJ plugin "Just Another Co-localization Plugin":
532 (https://imagej.nih.gov/ij/plugins/track/jacop2.html).
533
534 **ADDITIONAL RESOURCES**
535 None.
536
537

538 **Figure S1. Related to Figure 1. Stratification of *ACE2*, *TMPRSS2*, and *ADAM17***
539 **Expression in β cells by BMI.** β cell gene expression from eleven donors (ages 1-39 years)
540 from the HPAP scRNA-seq dataset (Kaestner et al., 2019) are displayed according to increasing
541 BMI. Only one donor had an obese BMI. (**A-B**) *ACE2* and *TMPRSS2* expression in β cells did
542 not show correlation with increasing BMI. (**C**) A trend towards increased *ADAM17* expression
543 with BMI was identified. However, only one obese donor was available and analyzed in this
544 dataset. Human pancreatic donor information is available in Table S2.
545
546 **Figure S2. Related to Figure 1 and 2. Testing and Characterization of Four ACE2-directed**
547 **Antibodies on Human Pancreatic Tissue.** (**A-E**) Characterization of ACE2 antibody (red,
548 ab15348) used by Yang et al. (Yang et al., 2020). Antibody epitope encompasses the ACE2 C-
549 terminal domain (human aa 788-805). Mouse kidney tissue served as a positive control for
550 ACE2 (**A**), while normal adult human pancreatic tissue incubated with anti-rabbit-Cy3 secondary
551 antibody only served as a negative control (**B**). Normal adult human pancreas labeled for ACE2
552 (red), INS (green, β cells) and GCG (blue, α cells) (**C-E**). Inset area is marked by a yellow box in
553 MERGE column. (**F-I**) Competition with immunizing peptide neutralized ACE2 labeling,
554 demonstrating the antibody's antigen specificity. Scale bars are 100 μm (**A-E**) and 50 μm (Inset,
555 **E** and **F-I**). (**J-N**) Characterization of ACE2 antibody (red, R&D MAB933) at same dilution (1:33)
556 reported by Fignani et al. (preprint: Fignani, 2020). Antibody epitope encompasses the ACE2
557 extracellular domain (human aa 18-740). Human kidney tissue served as a positive control for
558 ACE2 (**J**), while normal adult human pancreatic tissue incubated with anti-mouse-Cy3
559 secondary antibody only served as a negative control (**K**). Normal adult human pancreas
560 labeled for ACE2 (red), INS (green, β cells) and GCG (blue, α cells) (**L-N**). Inset area is marked
561 by a yellow box in MERGE column. Scale bars are 50 μm (**J-N**) and 25 μm (Inset, **N**). (**O-S**)
562 Characterization of ACE2 antibody (red, R&D AF933) at same dilution (1:200) reported by Yang

563 et al. (Yang et al., 2020). Antibody epitope encompasses the ACE2 extracellular domain
564 (human aa 18-740). Human kidney served as a positive control for ACE2 (**O**), while normal adult
565 human pancreatic tissue incubated with anti-goat-Cy3 secondary antibody only served as a
566 negative control (**P**). Normal adult human pancreas labeled for ACE2 (red), INS (green, β cells)
567 and GCG (blue, α cells) (**Q-S**). Inset area is marked by a yellow box in MERGE column. Scale
568 bars are 50 μm (**O-R**) and 25 μm (Inset, **S**). (**T-W**) Characterization of ACE2 antibody (red,
569 HPA000288) used by the Human Protein Atlas (Uhlen et al., 2015) and Hikmet et al. (Hikmet et
570 al., 2020). Antibody epitope encompasses the ACE2 extracellular domain (human aa 1-111).
571 Human kidney tissue served as a positive control for ACE2 (**T**). Normal adult human pancreas
572 labeled for ACE2 (red) and INS (green, β cells) (**U-W**). Inset area is marked by a white dashed
573 box in MERGE column. Scale bars are 100 μm (**T-V**) and 50 μm (Inset, **W**). DAPI (white).
574 Human pancreatic donor information is available in Table S2 (**B**, donor N8; **C-E**, donor N4; **F-I**,
575 donors N6 and N2; **J-N**, donor N2; **O-S**, donor N7; **T-W**, donor N8).
576
577 **Figure S3. Related to Figures 2 and 5. ACE2 and TMPRSS2 Protein are Not Detected by**
578 **Immunofluorescence in α or β Cells from Normal, T2D or T1D Adult Donors.** SARS-CoV-2
579 cell entry markers ACE2 (antibody ab15348) and TMPRSS2, both shown in red, are not
580 detected in islet α cells (GCG, blue) or β cells (INS, green) in pancreatic sections from adult
581 donors without diabetes (**A-H**) or donors with type 2 (**I-N**) or type 1 (**O-V**) diabetes. Insets are
582 depicted by a yellow box. DAPI (white). Scale bars are 100 μm (**A-V**) and 25 μm (Insets).
583 Human islet and pancreatic donor information is available in Table S2 (**A-D**, donors N3, N7, N9,
584 N8; **E-H**, donors N14, N12, N11, N10; **I-L**, donors 2L, 2B, 2G, 2I; **M-N**, donors 2H, 2G; **O-R**,
585 donors 1B, 1D, 1C, 1A; **S-V**, donors 1H, 1K, 1J, 1G).
586

587 **Figure S4. Related to Figures 1 and 2. DPP4 is Expressed in α cells of Adult Normal and**
588 **Diabetic Donors.** DPP4 (red) is expressed in human pancreatic islet α cells (GCG, blue;
589 Merged, magenta) but not β cells (INS, green) in pancreatic sections from adult donors without
590 diabetes (**A-C**) or donors with type 2 (**D-F**) or type 1 (**G-I**) diabetes. Scale bars are 50 μm (**A-I**).
591 Human islet and pancreatic donor information is available in Table S2 (**A-C**, donor N8; **D-F**,
592 donor 2K; **G-I**, donor 1H). (**J**) Dot plots of *ACE2*, *TMPRSS2*, *CTSL*, *ADAM17*, *FURIN*,
593 *TMPRSS4*, and *DPP4* expression compared with cell type-enriched genes from a previously
594 published single cell (sc) RNA-seq datasets (Camunas-Soler et al., 2020). Dot size indicates
595 percentage of cells in a given population expressing the gene; dot color represents scaled
596 average expression. Dotted line highlights *ACE2*, *TMPRSS2*, *CTSL*, *ADAM17*, *FURIN*,
597 *TMPRSS4*, and *DPP4* expression.
598
599 **Figure S5. Related to Figures 3 and 4. ACE2 is Localized to Islet and Exocrine Capillaries**
600 **in Adult Human Pancreas of T2D and T1D donors.** Representative images of endothelial
601 cells (CD31, white) and ACE2-positive perivascular cells (red; antibody ab15348) in islet (**A-H'**)
602 and exocrine tissue microvasculature (**I-P'**) of individuals with type 2 and type 1 diabetes. DAPI
603 (white). Yellow arrowheads point to CD31-positive endothelial cells, while magenta arrowheads
604 point to perivascular ACE2-positive cells. Insets (**A'-P'**) are depicted by yellow boxes in **A-P**.
605 ACE2 positive perivascular cells abut extracellular matrix marker collagen-IV within the vascular
606 basement membrane (collagen-IV [COL4], green; **D, D', H, H', L, L', P, P'**). ACE2 labeling was
607 reduced in both islets (**E-H'**) and exocrine tissue of individuals with type 1 diabetes (**M-P'**)
608 compared to normal donors (Figure 3) and those with type 2 diabetes. Scale bars are 50 μm (**A-**
609 **P**) and 10 μm (Insets, **A'-P'**). Human pancreatic donor information is available in Table S2 (**A-**
610 **D'**, donor 2E; **E-H'**, donor 1F; **I-L'**, donor 2E; **M-P'**, donor 1C).

611 **Table S1. Related to Figure 1. Number and Percentage of β cells that Express and Co-**

612 **express Putative SARS-CoV-2 Cell Entry Genes Across Four Independent scRNA-seq**

613 **Datasets.**

Genes	Droplet-based scRNA-seq				SMART-seq			
	HPAP[a] (β cell total, N=2828)		Baron et al.[b] (β cell total, N=2525)		Segerstolpe et al.[c] (β cell total, N=157)		Camunas-Soler et al.[c] (β cell total, N=357)	
	# β cell	% β cells	# β cell	% β cells	# β cell	% β cells	# β cell	% β cells
ACE2	17	0.6	4	0.2	3	1.9	12	3.4
TMPRSS2	60	2.1	7	0.3	4	2.5	2	0.6
TMPRSS4	0	0.0	0	0.0	0	0.0	9	2.5
CTSL	1421	50.2	977	38.7	132	84.1	291	81.5
FURIN	779	27.5	942	37.3	91	58.0	255	71.4
ADAM17	494	17.5	251	9.9	78	49.7	96	26.9
ACE2, TMPRSS2	0	0.0	0	0.0	0	0.0	0	0.0
ACE2,TMPRSS4	0	0.0	0	0.0	0	0.0	0	0.0
ACE2, CTSL	0	0.0	2	0.1	3	1.9	9	2.5
ACE2, FURIN	0	0.0	1	0.0	1	0.6	8	2.2
ACE2, ADAM17	0	0.0	0	0.0	1	0.6	3	0.8

614 [a]10x genomics; [b]InDrop (Klein et al., 2015); [c]SMART-seq2 (Picelli et al., 2014)

615

616

617

618

619

620

621

622

623

624

625

626

627

628

629 **Table S2. Related to STAR Methods. Demographic Information of Donors.**

Donor ID		Age	Ethnicity / Race	Diabetes Duration	Sex	BMI	Cause of Death	Tissue/Islet Source
Juvenile (Histology)	J1	5 days	Caucasian	--	F	14.9	Anoxia	IIAM
	J2	3 months	Caucasian	--	M	16.8	Anoxia	NDRI
	J3	10 months	Caucasian	--	F	15.4	CVA	NDRI
	J4	20 months	Caucasian	--	F	23.5	Anoxia	IIAM
	J5	5 years	Caucasian	--	M	16.2	Anoxia	IIAM
Normal Adult (Histology)	N1	42 years	Caucasian	--	M	32.2	Overdose	TNDS
	N2	45 years	Caucasian	--	F	29.7	Anoxia	OPO
	N3	46 years	Caucasian	--	F	32.9	CVA	IIAM
	N4	48 years	Caucasian	--	M	24.6	Anoxia	OPO
	N5	51 years	Caucasian	--	M	20.4	Anoxia	OPO
	N6	52 years	Black	--	M	29.2	ICH	TNDS
	N7	52 years	Caucasian	--	M	28.1	Head Trauma	OPO
	N8	55 years	Black	--	M	35.6	CVA	IIAM
	N9	59 years	Caucasian	--	M	32.7	Head Trauma	IIAM
	N10	20 years	Hispanic	--	M	19.4	Head Trauma	IIAM
	N11	24 years	Caucasian	--	M	35.5	ICH	IIAM
	N12	35 years	Caucasian	--	M	26.8	Head Trauma	IIAM
	N13	20 years	Caucasian	--	M	27.8	Head Trauma	NDRI
	N14	18 years	Caucasian	--	M	25.1	Head Trauma	IIAM
	HP1754	15 years	N/A	--	M	22.6	Head Trauma	IIAM
	HP2041	29 years	N/A	--	M	22.3	Head Trauma	IIAM
	HP2091	44 years	N/A	--	F	23.7	CVA	IIAM
Adult T1D (Histology)	1A	43 years	N/A	36 years	M	31.2	CVA	NDRI
	1B	45 years	Caucasian	43 years	M	25.0	Anoxia	IIAM
	1C	54 years	Caucasian	14 years	F	24.9	Anoxia	IIAM
	1D	57 years	Black	45 years	M	33.3	CVA	IIAM
	1E	58 years	Caucasian	31 years	M	21.8	Anoxia	NDRI
	1F	63 years	Caucasian	44 years	M	24.1	Anoxia	IIAM
	1G	35 years	Caucasian	23 years	M	26.9	Anoxia	NDRI
	1H	20 years	Caucasian	7 years	M	25.5	Anoxia	NDRI
	1I	27 years	Caucasian	17 years	M	18.4	Anoxia	NDRI
	1J	13 years	Caucasian	5 years	M	19.1	Anoxia	IIAM
	1K	30 years	Caucasian	20 years	M	29.8	Anoxia	NDRI
Adult T2D (Histology)	2A	44 years	Caucasian	7 years	M	44.4	CVA	IIAM
	2B	52 years	Caucasian	7 years	M	33.6	CVA	IIAM
	2C	52 years	Asian	10 years	F	21.9	CVA	NDRI
	2D	52 years	Caucasian	< 1 year	F	29.2	CVA	IIAM
	2E	42 years	Black	< 1 year	M	42.0	CVA	IIAM

	2F	43 years	Black	1 year	M	36.0	Head Trauma	IIAM
	2G	66 years	Caucasian	3 years	F	32.8	CVA	IIAM
	2H	47 years	Caucasian	3 years	M	31.3	CVA	IIAM
	2I	64 years	Caucasian	5 years	M	33.2	ICH	IIAM
	2J	59 years	Caucasian	6 years	F	27.5	CVA	IIAM
	2K	60 years	Caucasian	1 year	M	38.3	CVA	IIAM
	2L	49 years	Caucasian	3 years	F	33.8	CVA	IIAM
Normal Adult Islets (Gels and scRNA-Seq)	I1	40 years	Caucasian	--	F	30.8	Head Trauma	IIDP
	I2	41 years	N/A	--	M	20.3	N/A	IIDP
	I3	42 years	Caucasian	--	M	32.2	Overdose	IIDP
	HPAP022	39 years	Caucasian	--	F	34.7	Anoxia	HPAP
	HPAP026	24 years	Caucasian	--	M	20.8	Anoxia	HPAP
	HPAP034	13 years	Caucasian	--	M	18.6	Head Trauma	HPAP
	HPAP035	35 years	Caucasian	--	M	26.9	Anoxia	HPAP
	HPAP036	23 years	Caucasian	--	F	16	Head Trauma	HPAP
	HPAP037	35 years	Caucasian	--	F	21.9	CVA	HPAP
	HPAP039	5 years	Caucasian	--	F	16.3	Anoxia	HPAP
	HPAP040	35 years	Caucasian	--	M	23.9	CVA	HPAP
	HPAP042	1 year	Caucasian	--	M	17.9	Anoxia	HPAP
	HPAP044	3 years	Caucasian	--	F	12	Anoxia	HPAP
	HPAP047	8 years	Caucasian	--	M	16.8	CVA	HPAP
COVID-19 Patient Autopsy Samples (Histology)	1	82 years	Caucasian	--	M	26.8	ALI	VUMC Autopsy
	2	97 years	Caucasian	--	F	19.7	ALI	VUMC Autopsy
	3	81 years	Caucasian	>10 years[a]	M	23.3	ALI	VUMC Autopsy
	4	60 years	Hispanic	--	M	36.7	ALI	VUMC Autopsy
	5	51 years	Hispanic	23 years	M	29.4	ALI	VUMC Autopsy
	6	60 years	Caucasian	--	F	38.4	PE	VUMC Autopsy
	7	71 years	Black	Pre-existing[b]	M	31.5	ALI	VUMC Autopsy

ALI – acute lung injury; CVA, cerebrovascular accident; HPAP – Human Pancreas Analysis Program (Human Islet Research Network); ICH, intracerebral hemorrhage; IIAM – International Institute for the Advancement of Medicine; IIDP – Integrated Islet Distribution Program; N/A – not available; NDRI – National Disease Research Interchange; OPO – Organ Procurement Organization; PE – pulmonary embolism; T1D = type 1 diabetes; T2D – type 2 diabetes; TNDS – Tennessee Donor Services, Nashville; VUMC Autopsy – Vanderbilt University Medical Center Autopsy Pathology

[a]Oldest clinical patient note including diagnosis of diabetes mellitus was signed in 2010, suggesting disease duration of at least 10 years.

[b]Patient was prescribed an oral anti-diabetic medication confirming pre-existing diabetes diagnosis of unknown duration prior to admission with COVID-19.

630
631

632 **REFERENCES**

633 Aid, M., Busman-Sahay, K., Vidal, S., Maliga, Z., Bondoc, S., Starke, C., Terry, M., Jacobson,
634 C., Wrijil, L., Ducat, S., Brook, O., Miller, A., Porto, M., Pellegrini, K., Pino, M., Hoang, T.,
635 Chandrashekar, A., Patel, S., Stephenson, K., Bosinger, S., Andersen, H., Lewis, M., Hecht, J.,
636 Sorger, P., Martinot, A., Estes, J., Barouch, D. (2020). Vascular disease and thrombosis in
637 SARS-CoV-2 infected Rhesus macaques. Cell *In Press*.

638 Almaca, J., Caicedo, A., and Landsman, L. (2020). Beta cell dysfunction in diabetes: the islet
639 microenvironment as an unusual suspect. Diabetologia *63*, 2076-2085.

640 Almaca, J., Weitz, J., Rodriguez-Diaz, R., Pereira, E., and Caicedo, A. (2018). The pericyte of
641 the pancreatic islet regulates capillary diameter and local blood flow. Cell Metab *27*, 630-644
642 e634.

643 Apicella, M., Campopiano, M.C., Mantuano, M., Mazoni, L., Coppelli, A., and Del Prato, S.
644 (2020). COVID-19 in people with diabetes: understanding the reasons for worse outcomes.
645 Lancet Diabetes Endocrinol.

646 Arda, H.E., Li, L., Tsai, J., Torre, E.A., Rosli, Y., Peiris, H., Spitale, R.C., Dai, C., Gu, X., Qu, K.,
647 et al. (2016). Age-dependent pancreatic gene regulation reveals mechanisms governing human
648 beta cell function. Cell Metab *23*, 909-920.

649 Ashok, A., Faghih, M., and Singh, V.K. (2020). Mild pancreatic enzyme elevations in COVID-19
650 pneumonia: synonymous with injury or noise? Gastroenterology.

651 Balamurugan, A.N., Gu, Y., Miyamoto, M., Wang, W., Inoue, K., and Tabata, Y. (2003).
652 Isolation, culture, and functional characteristics of diabetic islets [corrected]. Pancreas *26*, 102-
653 103.

654 Baron, M., Veres, A., Wolock, S.L., Faust, A.L., Gaujoux, R., Vetere, A., Ryu, J.H., Wagner,
655 B.K., Shen-Orr, S.S., Klein, A.M., et al. (2016). A single-cell transcriptomic map of the human
656 and mouse pancreas reveals inter- and intra-cell population structure. Cell Syst *3*, 346-360
657 e344.

658 Barron, E., Bakhai, C., Kar, P., Weaver, A., Bradley, D., Ismail, H., Knighton, P., Holman, N.,
659 Khunti, K., Sattar, N., et al. (2020). Associations of type 1 and type 2 diabetes with COVID-19-
660 related mortality in England: a whole-population study. Lancet Diabetes Endocrinol *8*, 813-822.

661 Blodgett, D.M., Nowosielska, A., Afik, S., Pechhold, S., Cura, A.J., Kennedy, N.J., Kim, S.,
662 Kucukural, A., Davis, R.J., Kent, S.C., et al. (2015). Novel observations from next-generation
663 RNA sequencing of highly purified human adult and fetal islet cell subsets. Diabetes *64*, 3172-
664 3181.

665 Bonney, G.K., Gao, Y., Chew, C.A., and Windsor, J.A. (2020). SARS-COV-2 associated acute
666 pancreatitis: Cause, consequence or epiphenomenon? Pancreatology.

667 Bornstein, S.R., Rubino, F., Khunti, K., Mingrone, G., Hopkins, D., Birkenfeld, A.L., Boehm, B.,
668 Amiel, S., Holt, R.I., Skyler, J.S., et al. (2020). Practical recommendations for the management
669 of diabetes in patients with COVID-19. Lancet Diabetes Endocrinol *8*, 546-550.

670 Breidenbach, J.D., Dube, P., Ghosh, S., Abdullah, B.N., Modyanov, N.N., Malhotra, D., Dworkin,
671 L.D., Haller, S.T., and Kennedy, D.J. (2020). Impact of Comorbidities on SARS-CoV-2 Viral
672 Entry-Related Genes. J Pers Med *10*.

673 Brissova, M., Aamodt, K., Brahmachary, P., Prasad, N., Hong, J.Y., Dai, C., Mellati, M.,
674 Shostak, A., Poffenberger, G., Aramandla, R., et al. (2014). Islet microenvironment, modulated
675 by vascular endothelial growth factor-A signaling, promotes beta cell regeneration. Cell Metab
676 *19*, 498-511.

677 Brissova, M., Fowler, M.J., Nicholson, W.E., Chu, A., Hirshberg, B., Harlan, D.M., and Powers,
678 A.C. (2005). Assessment of human pancreatic islet architecture and composition by laser
679 scanning confocal microscopy. J Histochem Cytochem *53*, 1087-1097.

680 Brissova, M., Haliyur, R., Saunders, D., Shrestha, S., Dai, C., Blodgett, D.M., Bottino, R.,
681 Campbell-Thompson, M., Aramandla, R., Poffenberger, G., et al. (2018). alpha Cell Function
682 and Gene Expression Are Compromised in Type 1 Diabetes. Cell Rep *22*, 2667-2676.

683 Bruno, G., Fabrizio, C., Santoro, C.R., and Buccoliero, G.B. (2020). Pancreatic injury in the
684 course of coronavirus disease 2019: A not-so-rare occurrence. J Med Virol.

685 Camunas-Soler, J., Dai, X.Q., Hang, Y., Bautista, A., Lyon, J., Suzuki, K., Kim, S.K., Quake,
686 S.R., and MacDonald, P.E. (2020). Patch-seq links single-cell transcriptomes to human islet
687 dysfunction in diabetes. Cell Metab *31*, 1017-1031 e1014.

688 Cariou, B., Hadjadj, S., Wargny, M., Pichelin, M., Al-Salameh, A., Allix, I., Amadou, C., Arnault,
689 G., Baudoux, F., Bauduceau, B., et al. (2020). Phenotypic characteristics and prognosis of
690 inpatients with COVID-19 and diabetes: the CORONADO study. Diabetologia *63*, 1500-1515.

691 Chee, Y.J., Ng, S.J.H., and Yeoh, E. (2020). Diabetic ketoacidosis precipitated by Covid-19 in a
692 patient with newly diagnosed diabetes mellitus. Diabetes Res Clin Pract *164*, 108166.

693 Chen, L., Li, X., Chen, M., Feng, Y., and Xiong, C. (2020). The ACE2 expression in human
694 heart indicates new potential mechanism of heart injury among patients infected with SARS-
695 CoV-2. Cardiovasc Res *116*, 1097-1100.

696 Clausen, T.M., Sandoval, D.R., Spliid, C.B., Pihl, J., Perrett, H.R., Painter, C.D., Narayanan, A.,
697 Majowicz, S.A., Kwong, E.M., McVicar, R.N., et al. (2020). SARS-CoV-2 Infection Depends on
698 Cellular Heparan Sulfate and ACE2. Cell.

699 Dai, C., Hang, Y., Shostak, A., Poffenberger, G., Hart, N., Prasad, N., Phillips, N., Levy, S.E.,
700 Greiner, D.L., Shultz, L.D., et al. (2017). Age-dependent human beta cell proliferation induced
701 by glucagon-like peptide 1 and calcineurin signaling. J Clin Invest *127*, 3835-3844.

702 Drucker, D.J. (2020). Coronavirus infections and type 2 diabetes-shared pathways with
703 therapeutic implications. Endocr Rev *41*.

704 Filippi, C.M., and von Herrath, M.G. (2008). Viral trigger for type 1 diabetes: pros and cons.
705 Diabetes *57*, 2863-2871.

706 Goldman, N., Fink, D., Cai, J., Lee, Y.N., and Davies, Z. (2020). High prevalence of COVID-19-
707 associated diabetic ketoacidosis in UK secondary care. Diabetes Res Clin Pract *166*, 108291.

708 Gupta, A., Madhavan, M.V., Sehgal, K., Nair, N., Mahajan, S., Sehrawat, T.S., Bikdeli, B.,
709 Ahluwalia, N., Ausiello, J.C., Wan, E.Y., et al. (2020). Extrapulmonary manifestations of COVID-
710 19. Nat Med *26*, 1017-1032.

711 Hamming, I., Timens, W., Bulthuis, M.L., Lely, A.T., Navis, G., and van Goor, H. (2004). Tissue
712 distribution of ACE2 protein, the functional receptor for SARS coronavirus. A first step in
713 understanding SARS pathogenesis. J Pathol *203*, 631-637.

714 He, L., Mae, M., Sun, Y., Muhl, L, Nahar, K., et al (2020). Pericyte-specific vascular expression
715 of SARS-CoV-2 receptor ACE2 – implications for microvascular inflammation and
716 hypercoagulopathy in COVID-19 patients. Biorxiv.

717 Heaney, A.I., Griffin, G.D., and Simon, E.L. (2020). Newly diagnosed diabetes and diabetic
718 ketoacidosis precipitated by COVID-19 infection. Am J Emerg Med.

719 Hikmet, F., Mear, L., Edvinsson, A., Micke, P., Uhlen, M., and Lindskog, C. (2020). The protein
720 expression profile of ACE2 in human tissues. Mol Syst Biol *16*, e9610.

721 Hoffmann, M., Kleine-Weber, H., Schroeder, S., Kruger, N., Herrler, T., Erichsen, S.,
722 Schiergens, T.S., Herrler, G., Wu, N.H., Nitsche, A., et al. (2020). SARS-CoV-2 cell entry
723 depends on ACE2 and TMPRSS2 and is blocked by a clinically proven protease inhibitor. Cell
724 *181*, 271-280 e278.

725 Hollstein, T., Schulte, D.M., Schulz, J., Gluck, A., Ziegler, A.G., Bonifacio, E., Wendorff, M.,
726 Franke, A., Schreiber, S., Bornstein, S.R., et al. (2020). Autoantibody-negative insulin-
727 dependent diabetes mellitus after SARS-CoV-2 infection: a case report. Nat Metab.

728 Holman, N., Knighton, P., Kar, P., O'Keefe, J., Curley, M., Weaver, A., Barron, E., Bakhai, C.,
729 Khunti, K., Wareham, N.J., et al. (2020). Risk factors for COVID-19-related mortality in people
730 with type 1 and type 2 diabetes in England: a population-based cohort study. Lancet Diabetes
731 Endocrinol *8*, 823-833.

732 Kaestner, K.H., Powers, A.C., Naji, A., Consortium, H., and Atkinson, M.A. (2019). NIH Initiative
733 to Improve Understanding of the Pancreas, Islet, and Autoimmunity in Type 1 Diabetes: The
734 Human Pancreas Analysis Program (HPAP). Diabetes *68*, 1394-1402.

735 Karimzadeh, S., Manzuri, A., Ebrahimi, M., and Huy, N.T. (2020). COVID-19 presenting as
736 acute pancreatitis: Lessons from a patient in Iran. Pancreatology.

737 Kim, N.Y., Ha, E., Moon, J.S., Lee, Y.H., and Choi, E.Y. (2020). Acute hyperglycemic crises with
738 coronavirus disease-19: case reports. Diabetes Metab J *44*, 349-353.

739 Klein, A.M., Mazutis, L., Akartuna, I., Tallapragada, N., Veres, A., Li, V., Peshkin, L., Weitz,
740 D.A., and Kirschner, M.W. (2015). Droplet barcoding for single-cell transcriptomics applied to
741 embryonic stem cells. Cell *161*, 1187-1201.

742 Koch, M., Holmes, D., Bennet, N. (2020). COVID-19 and diabetes: a co-conspiracy? Lancet
743 Diabetes Endocrinol *8*, 801.

744 Kusmartseva, I., Wu, W., Syed, F., Van Der Heide, V., Jorgensen, M., Joseph, P., Tang, X.,
745 Candelario-Jalil, E., Yang, C., Nick, H., Harbert, J., Posgai, A., Lloyd, R., Cechin, S., Pugliese,
746 A., Campbell-Thompson, M., Vander Heide, R., Evans-Molina, C., Homann, D., Atkinson, M.
747 (2020). ACE2 and SARS-CoV-2 Expression in the Normal and COVID-19 Pancreas. Biorxiv.

748 Lan, J., Ge, J., Yu, J., Shan, S., Zhou, H., Fan, S., Zhang, Q., Shi, X., Wang, Q., Zhang, L., et
749 al. (2020). Structure of the SARS-CoV-2 spike receptor-binding domain bound to the ACE2
750 receptor. Nature *581*, 215-220.

751 Lee, I.T., Nakayama, T., Wu, C.T., Goltsev, Y., Jiang, S., Gall, P.A., Liao, C.K., Shih, L.C.,
752 Schurch, C.M., McIlwain, D.R., et al. (2020). Robust ACE2 protein expression localizes to the
753 motile cilia of the respiratory tract epithelia and is not increased by ACE inhibitors or angiotensin
754 receptor blockers. medRxiv.

755 Li, J., Wang, X., Chen, J., Zuo, X., Zhang, H., and Deng, A. (2020a). COVID-19 infection may
756 cause ketosis and ketoacidosis. Diabetes Obes Metab.

757 Li, Y., Zhang, Z., Yang, L., Lian, X., Xie, Y., Li, S., Xin, S., Cao, P., and Lu, J. (2020b). The
758 MERS-CoV receptor DPP4 as a candidate binding target of the SARS-CoV-2 spike. iScience
759 *23*, 101160.

760 Meireles, P.A., Bessa, F., Gaspar, P., Parreira, I., Silva, V.D., Mota, C., and Alvoeiro, L. (2020).
761 Acalculous acute pancreatitis in a COVID-19 patient. Eur J Case Rep Intern Med *7*, 001710.

762 Nair, G.G., Liu, J.S., Russ, H.A., Tran, S., Saxton, M.S., Chen, R., Juang, C., Li, M.L., Nguyen,
763 V.Q., Giacometti, S., et al. (2019). Recapitulating endocrine cell clustering in culture promotes
764 maturation of human stem-cell-derived beta cells. Nat Cell Biol *21*, 263-274.

765 Picelli, S., Faridani, O.R., Bjorklund, A.K., Winberg, G., Sagasser, S., and Sandberg, R. (2014).
766 Full-length RNA-seq from single cells using Smart-seq2. Nat Protoc *9*, 171-181.

767 preprint: Fignani, D., Licata, G., Brusco, N., Nigi, L., Grieco, G., Marselli, L., Overbergh, L.,
768 Gysemans, C., Colli, M., Marchetti, P., Mathieu, C., Eizirik, D., Sebastiani, G., Dotta, F. (2020).
769 SARS-CoV-2 receptor angiotensin I-converting enzyme type 2 is expressed in human
770 pancreatic islet β-cells and is upregulated by inflammatory stress. BioRxiv.

771 Rabice, S.R., Altshuler, P.C., Bovet, C., Sullivan, C., and Gagnon, A.J. (2020). COVID-19
772 infection presenting as pancreatitis in a pregnant woman: A case report. Case Rep Womens
773 Health *27*, e00228.

774 Rafique, S., and Ahmed, F.W. (2020). A Case of Combined Diabetic Ketoacidosis and
775 Hyperosmolar Hyperglycemic State in a Patient With COVID-19. Cureus *12*, e8965.

776 Riddle, M.C., Buse, J.B., Franks, P.W., Knowler, W.C., Ratner, R.E., Selvin, E., Wexler, D.J.,
777 and Kahn, S.E. (2020). COVID-19 in people with diabetes: urgently needed lessons from early
778 reports. Diabetes Care *43*, 1378-1381.

779 Schreiber, B., Patel, A., and Verma, A. (2020). Shedding Light on COVID-19: ADAM17 the
780 Missing Link? Am J Ther.

781 Segerstolpe, A., Palasantza, A., Eliasson, P., Andersson, E.M., Andreasson, A.C., Sun, X.,
782 Picelli, S., Sabirsh, A., Clausen, M., Bjursell, M.K., et al. (2016). Single-cell transcriptome
783 profiling of human pancreatic islets in health and type 2 diabetes. Cell Metab *24*, 593-607.

784 Seyedpour, S., Khodaei, B., Loghman, A.H., Seyedpour, N., Kisomi, M.F., Balibegloo, M.,
785 Nezamabadi, S.S., Gholami, B., Saghazadeh, A., and Rezaei, N. (2020). Targeted therapy
786 strategies against SARS-CoV-2 cell entry mechanisms: A systematic review of in vitro and in
787 vivo studies. J Cell Physiol.

788 Shang, J., Wan, Y., Luo, C., Ye, G., Geng, Q., Auerbach, A., and Li, F. (2020). Cell entry
789 mechanisms of SARS-CoV-2. Proc Natl Acad Sci U S A *117*, 11727-11734.

790 Stuart, T., Butler, A., Hoffman, P., Hafemeister, C., Papalexi, E., Mauck, W.M., 3rd, Hao, Y.,
791 Stoeckius, M., Smibert, P., and Satija, R. (2019). Comprehensive Integration of Single-Cell
792 Data. Cell *177*, 1888-1902 e1821.

793 Taneera, J., El-Huneidi, W., Hamad, M., Mohammed, A.K., Elaraby, E., and Hachim, M.Y.
794 (2020). Expression Profile of SARS-CoV-2 Host Receptors in Human Pancreatic Islets
795 Revealed Upregulation of ACE2 in Diabetic Donors. Biology (Basel) *9*.

796 Teuwen, L.A., Geldhof, V., Pasut, A., and Carmeliet, P. (2020). COVID-19: the vasculature
797 unleashed. Nat Rev Immunol *20*, 389-391.

798 Uhlen, M., Fagerberg, L., Hallstrom, B.M., Lindskog, C., Oksvold, P., Mardinoglu, A., Sivertsson,
799 A., Kampf, C., Sjostedt, E., Asplund, A., et al. (2015). Proteomics. Tissue-based map of the
800 human proteome. Science *347*, 1260419.

801 Unsworth, R., Wallace, S., Oliver, N.S., Yeung, S., Kshirsagar, A., Naidu, H., Kwong, R.M.W.,
802 Kumar, P., and Logan, K.M. (2020). New-Onset Type 1 Diabetes in Children During COVID-19:
803 Multicenter Regional Findings in the U.K. Diabetes Care.

804 van den Brink, S.C., Sage, F., Vertesy, A., Spanjaard, B., Peterson-Maduro, J., Baron, C.S.,
805 Robin, C., and van Oudenaarden, A. (2017). Single-cell sequencing reveals dissociation-
806 induced gene expression in tissue subpopulations. Nat Methods *14*, 935-936.

807 Vankadari, N., and Wilce, J.A. (2020). Emerging WuHan (COVID-19) coronavirus: glycan shield
808 and structure prediction of spike glycoprotein and its interaction with human CD26. Emerg
809 Microbes Infect *9*, 601-604.

810 Wang, F., Wang, H., Fan, J., Zhang, Y., Wang, H., and Zhao, Q. (2020). Pancreatic injury
811 patterns in patients with coronavirus disease 19 pneumonia. Gastroenterology *159*, 367-370.

812 Wang, S., Ma, P., Zhang, S., Song, S., Wang, Z., Ma, Y., Xu, J., Wu, F., Duan, L., Yin, Z., Luo,
813 H., Xiong, N., Xu, M., Zeng, T., Jin, Y. (2020). Fasting blood glucose at admission is an
814 independent predictor for 28-day mortality in patients with COVID-19 without previous diagnosis
815 of diabetes: a multi-centre retrospective study. Diabetologia.

816 Wiersinga, W.J., Rhodes, A., Cheng, A.C., Peacock, S.J., and Prescott, H.C. (2020).
817 Pathophysiology, Transmission, Diagnosis, and Treatment of Coronavirus Disease 2019
818 (COVID-19): A Review. JAMA.

819 Wright, J.J., Saunders, D.C., Dai, C., Poffenberger, G., Cairns, B., Serreze, D.V., Harlan, D.M.,
820 Bottino, R., Brissova, M., and Powers, A.C. (2020). Decreased pancreatic acinar cell number in
821 type 1 diabetes. Diabetologia *63*, 1418-1423.

822 Yang, J.K., Lin, S.S., Ji, X.J., and Guo, L.M. (2010). Binding of SARS coronavirus to its receptor
823 damages islets and causes acute diabetes. Acta Diabetol *47*, 193-199.

824 Yang, L., Han, Y., Nilsson-Payant, B.E., Gupta, V., Wang, P., Duan, X., Tang, X., Zhu, J., Zhao,
825 Z., Jaffre, F., et al. (2020). A human pluripotent stem cell-based platform to study SARS-CoV-2
826 tropism and model virus infection in human cells and organoids. Cell Stem Cell *27*, 125-136
827 e127.

828 Zang, R., Gomez Castro, M.F., McCune, B.T., Zeng, Q., Rothlauf, P.W., Sonnek, N.M., Liu, Z.,
829 Brulois, K.F., Wang, X., Greenberg, H.B., et al. (2020). TMPRSS2 and TMPRSS4 promote
830 SARS-CoV-2 infection of human small intestinal enterocytes. Sci Immunol *5*.

831 Zhou, F., Yu, T., Du, R., Fan, G., Liu, Y., Liu, Z., Xiang, J., Wang, Y., Song, B., Gu, X., et al.
832 (2020). Clinical course and risk factors for mortality of adult inpatients with COVID-19 in Wuhan,
833 China: a retrospective cohort study. Lancet *395*, 1054-1062.
834

Figure 1

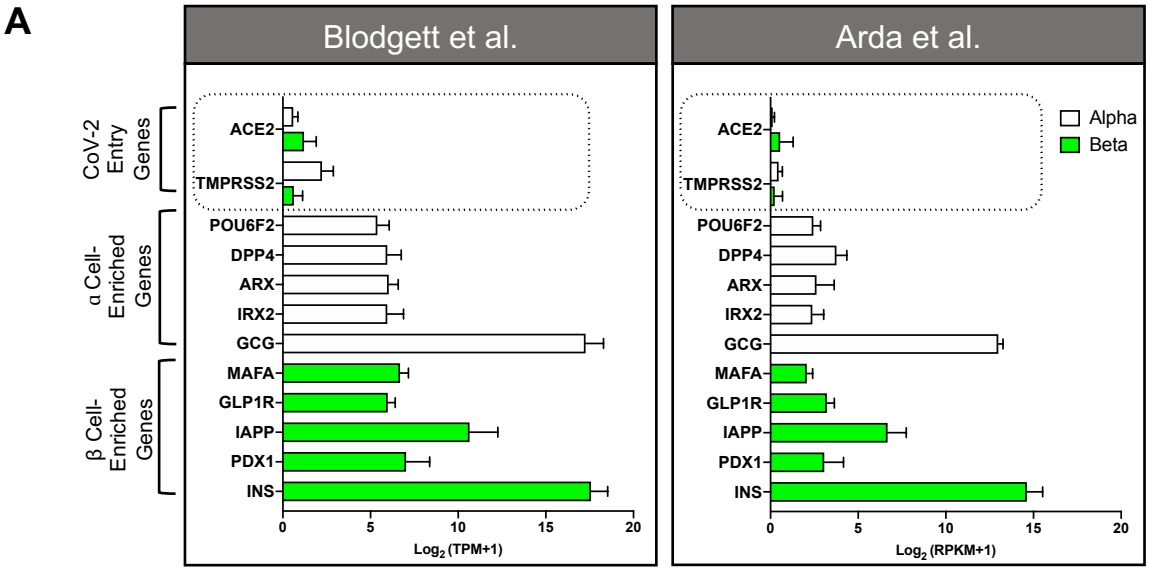
A
Blodgett et al.
Arda et al.
CoV-2 Entry Genes
α Cell-Enriched Genes
β Cell-Enriched Genes
ACE2
TMPRSS2
POU6F2
DPP4
ARX
IRX2
GCG
MAFA
GLP1R
IAPP
PDX1
INS
Alpha
Beta
Log2 (TPM+1)
Log2 (RPKM+1)

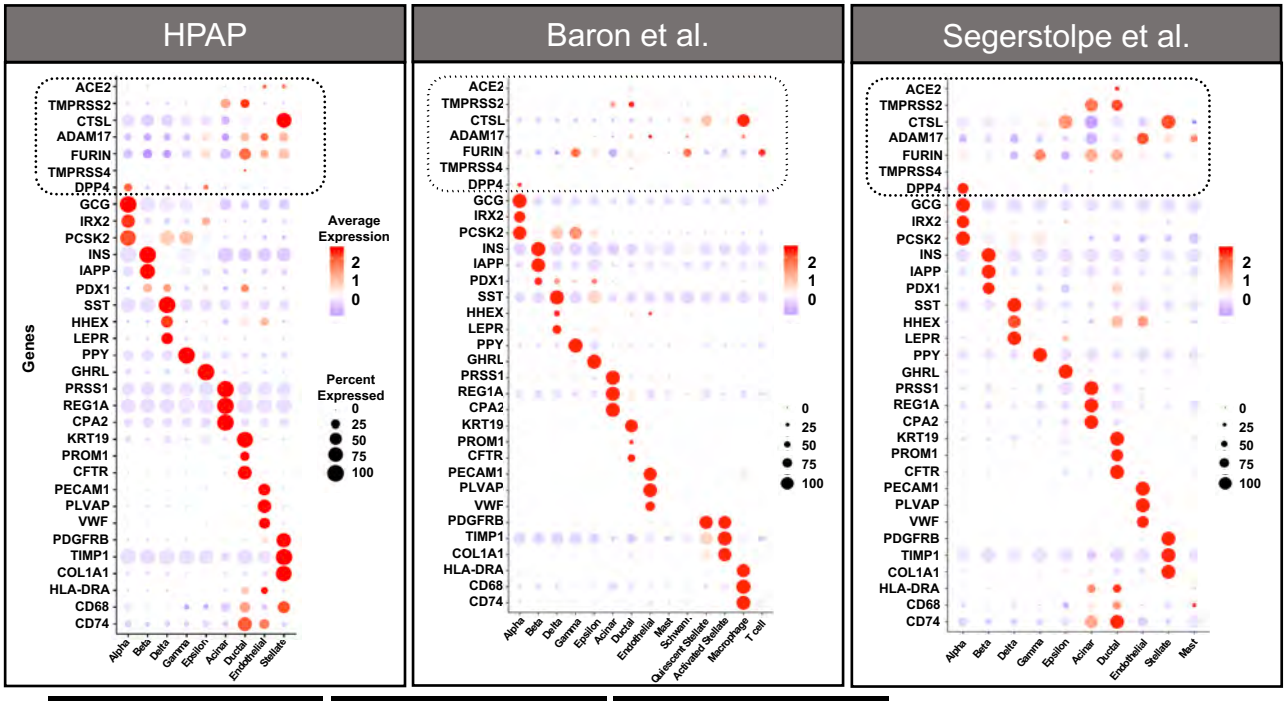
B
HPAP
Baron et al.
Segerstolpe et al.
Genes
Average Expression
Percent Expressed
ACE2
TMPRSS2
CTSL
ADAM17
FURIN
TMPRSS4
DPP4
GCG
IRX2
PCSK2
INS
IAPP
PDX1
SST
HHEX
LEPR
PPY
GHRL
PRSS1
REG1A
CPA2
KRT19
PROM1
CFTR
PECAM1
PLVAP
VWF
PDGFRB
TIMP1
COL1A1
HLA-DRA
CD68
CD74
Alpha
Beta
Delta
Gamma
Epsilon
Acinar
Ductal
Endothelial
Mast
Stellate

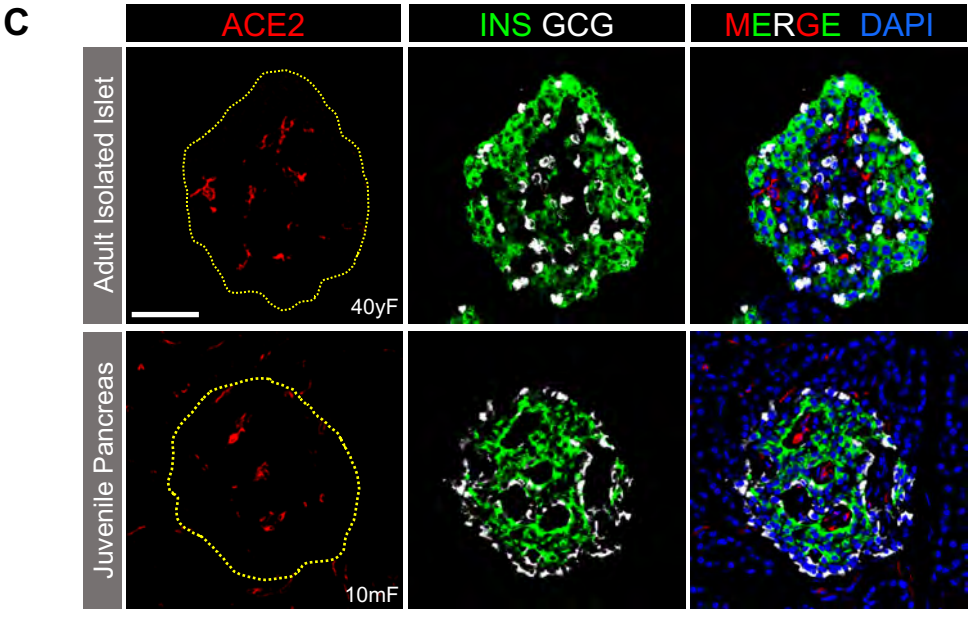
C
ACE2
INS GCG
MERGE DAPI
Adult Isolated Islet
Juvenile Pancreas
40yF
10mF

Figure 2

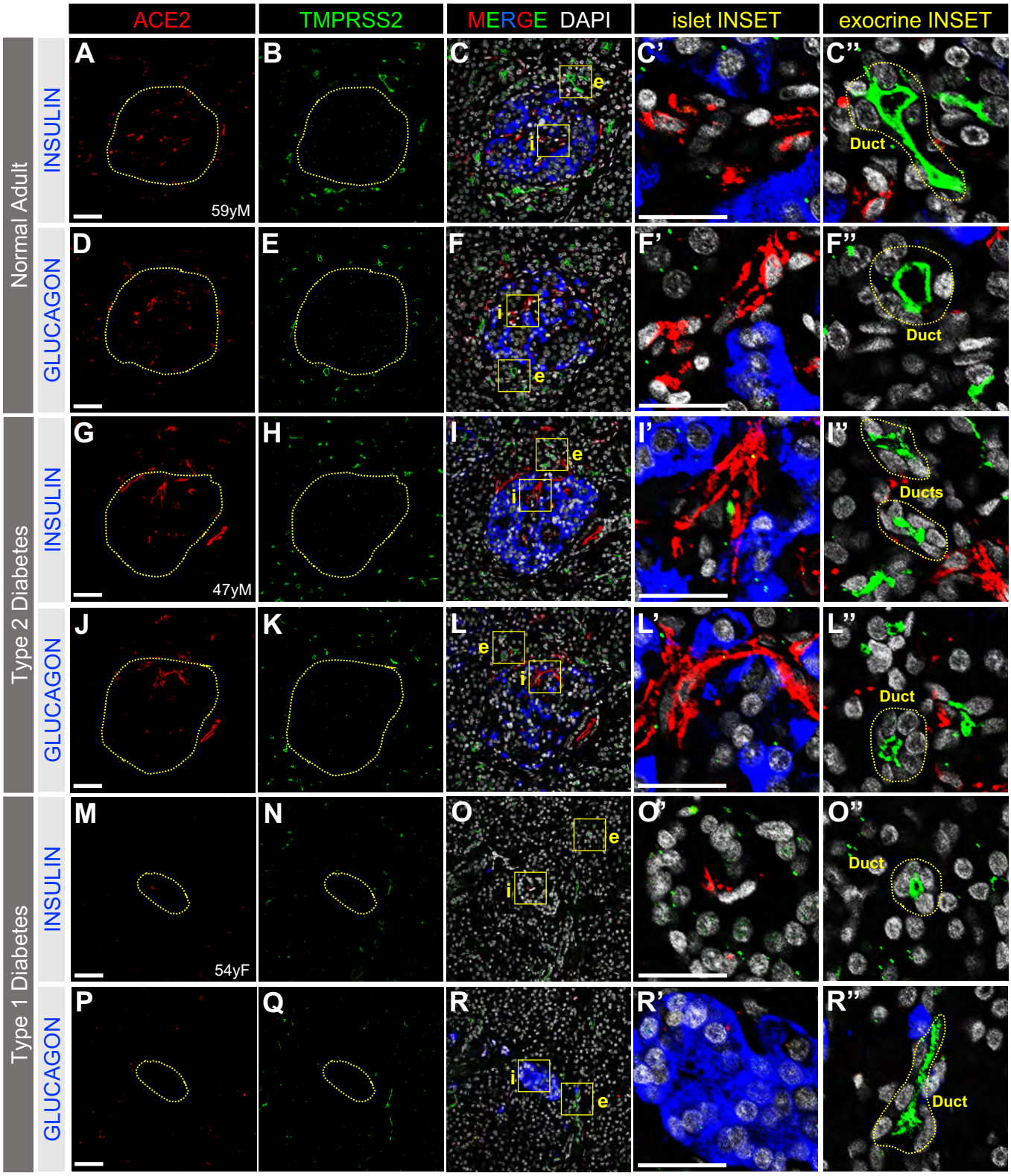
ACE2
TMPRSS2
MERGE DAPI
islet INSET
exocrine INSET
Normal Adult
INSULIN
GLUCAGON
Type 2 Diabetes
INSULIN
GLUCAGON
Type 1 Diabetes
INSULIN
GLUCAGON
A
B
C
C'
C''
D
E
F
F'
F''
G
H
I
I'
I''
J
K
L
L'
L''
M
N
O
O'
O''
P
Q
R
R'
R''
59yM
47yM
54yF
e
i
Duct
Ducts

Figure 3

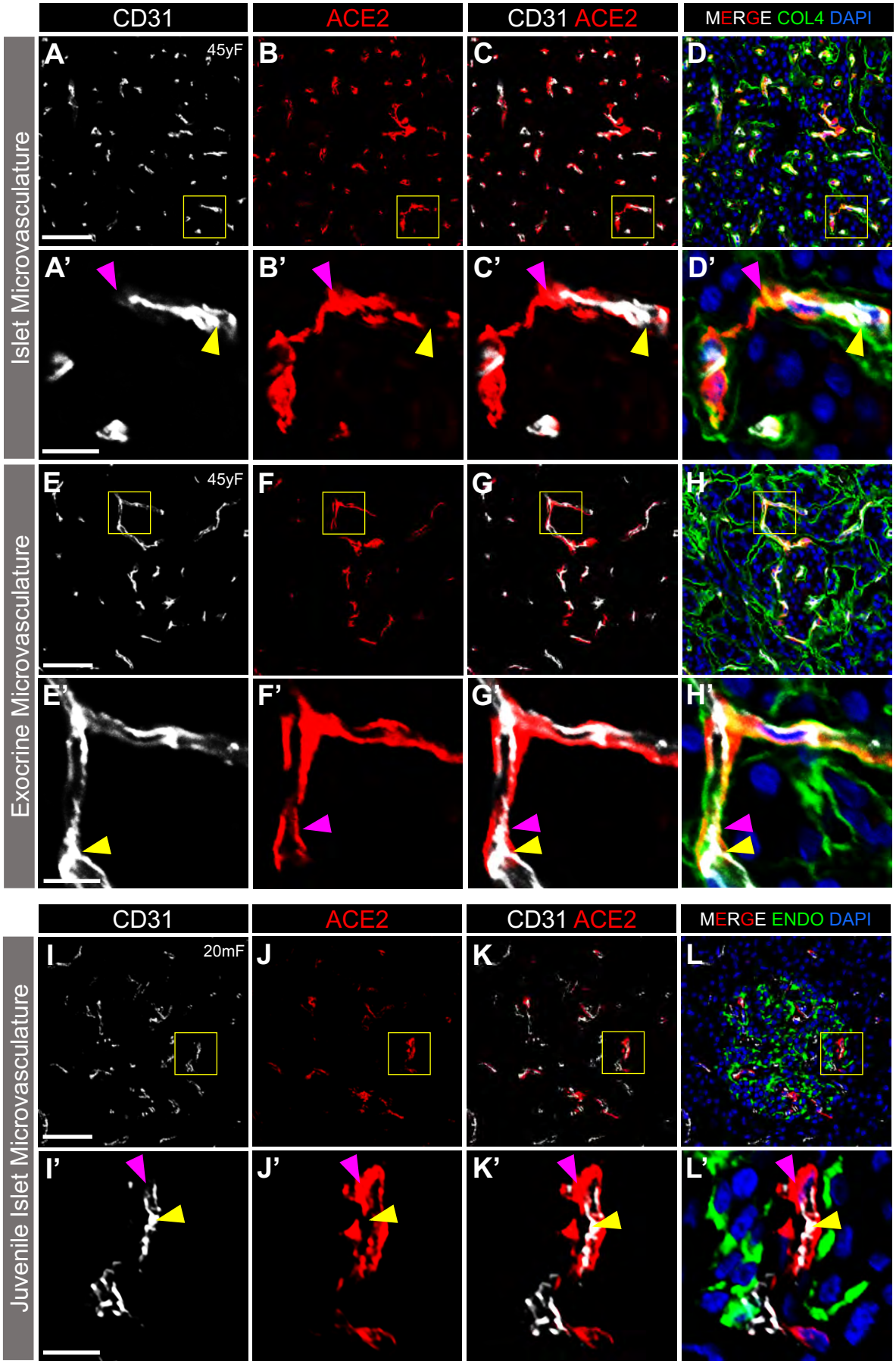
CD31
ACE2
CD31 ACE2
MERGE COL4 DAPI
Islet Microvasculature
A
45yF
B
C
D
A'
B'
C'
D'
Exocrine Microvasculature
E
45yF
F
G
H
E'
F'
G'
H'
CD31
ACE2
CD31 ACE2
MERGE ENDO DAPI
Juvenile Islet Microvasculature
I
20mF
J
K
L
I'
J'
K'
L'

Figure 4

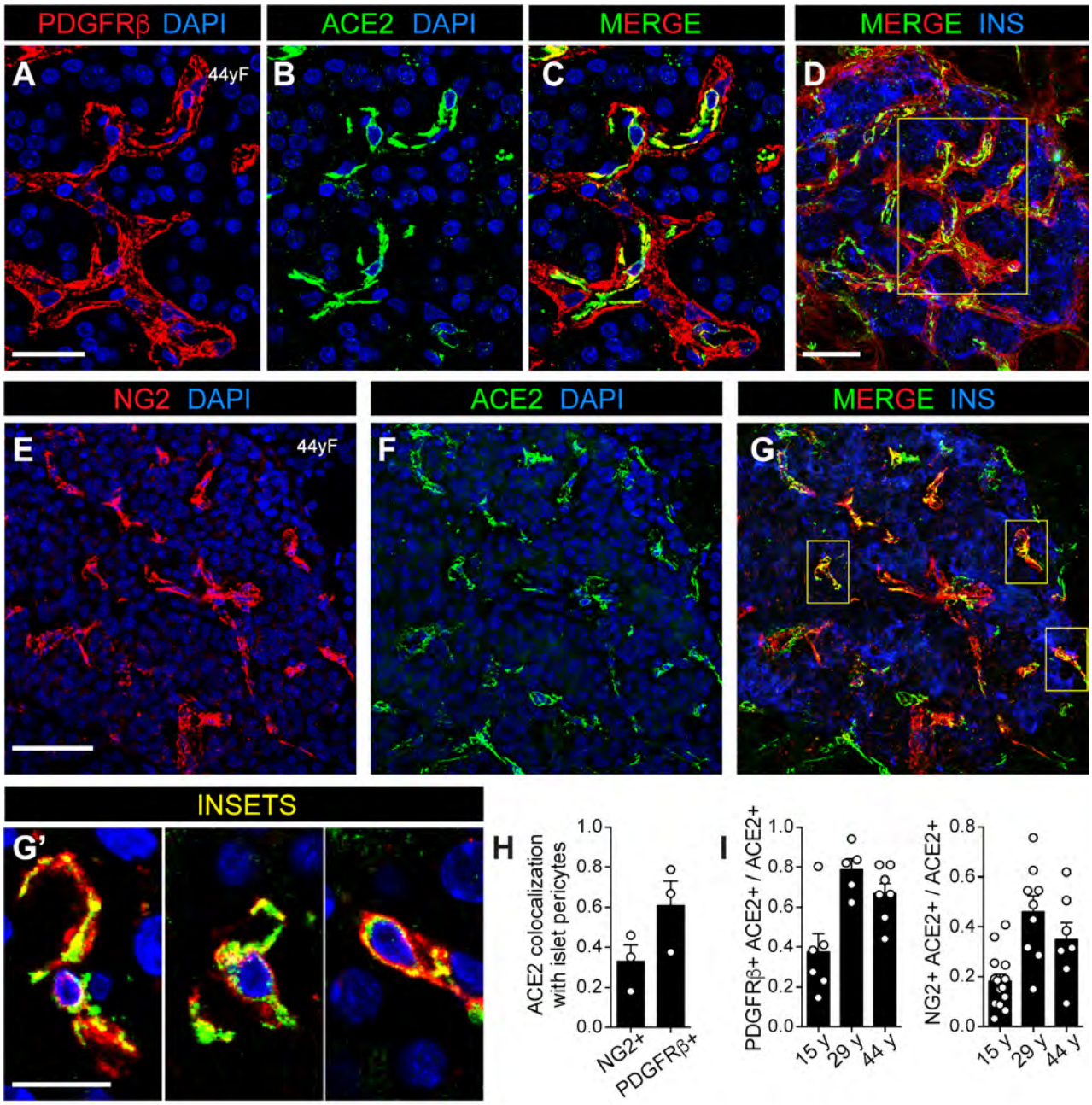
PDGFRβ DAPI
ACE2 DAPI
MERGE
MERGE INS
A
44yF
B
C
D
NG2 DAPI
ACE2 DAPI
MERGE INS
E
44yF
F
G
INSETS
G'
H
ACE2 colocalization with islet pericytes
1.0
0.8
0.6
0.4
0.2
0.0
NG2+
PDGFRβ+
I
PDGFRβ+ ACE2+ / ACE2+
NG2+ ACE2+ / ACE2+
15 y
29 y
44 y

Figure 5

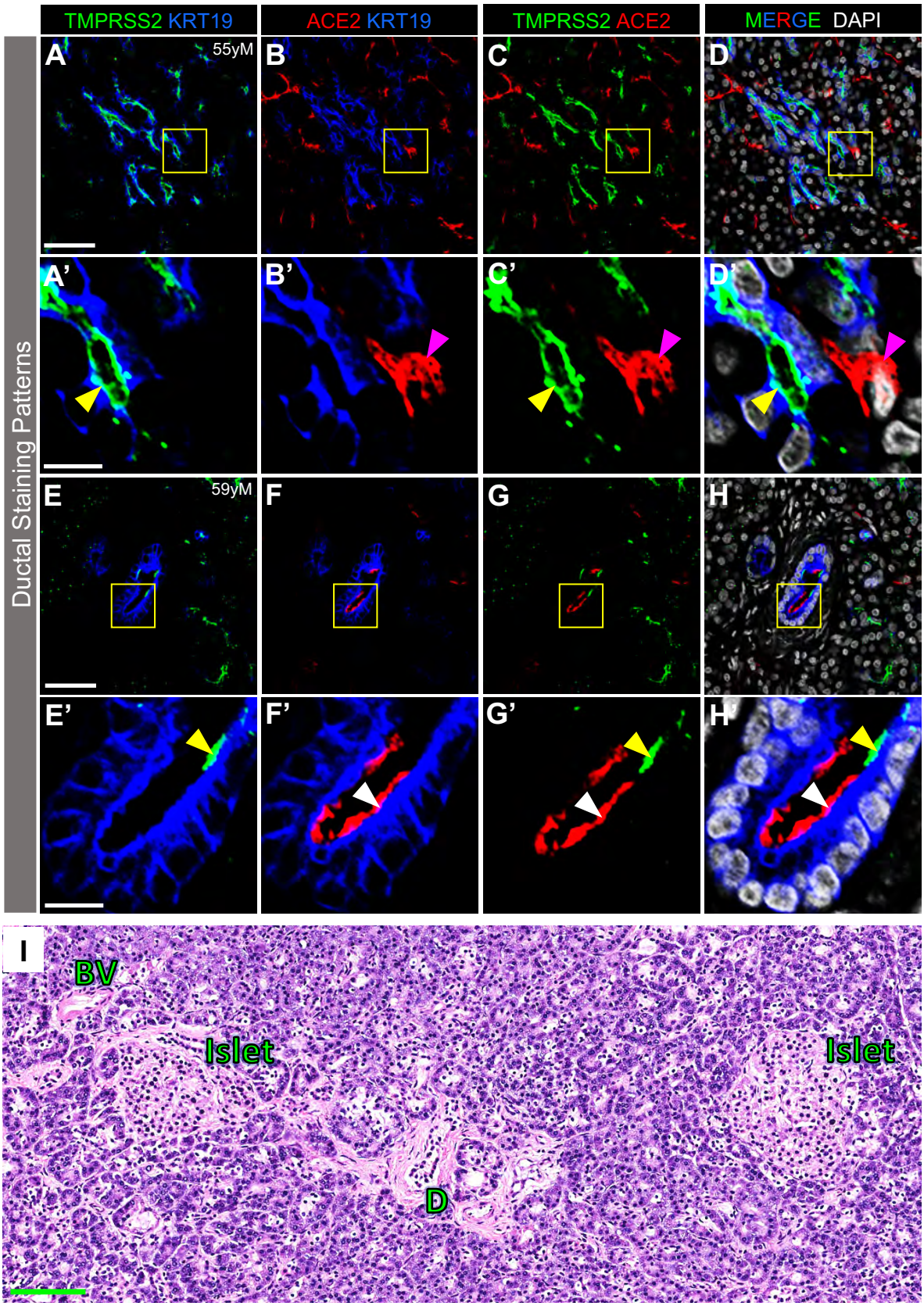
TMPRSS2 KRT19
ACE2 KRT19
TMPRSS2 ACE2
MERGE DAPI
Ductal Staining Patterns
A
55yM
B
C
D
A'
B'
C'
D'
E
59yM
F
G
H
E'
F'
G'
H'
I
BV
Islet
Islet
D

Figure S1

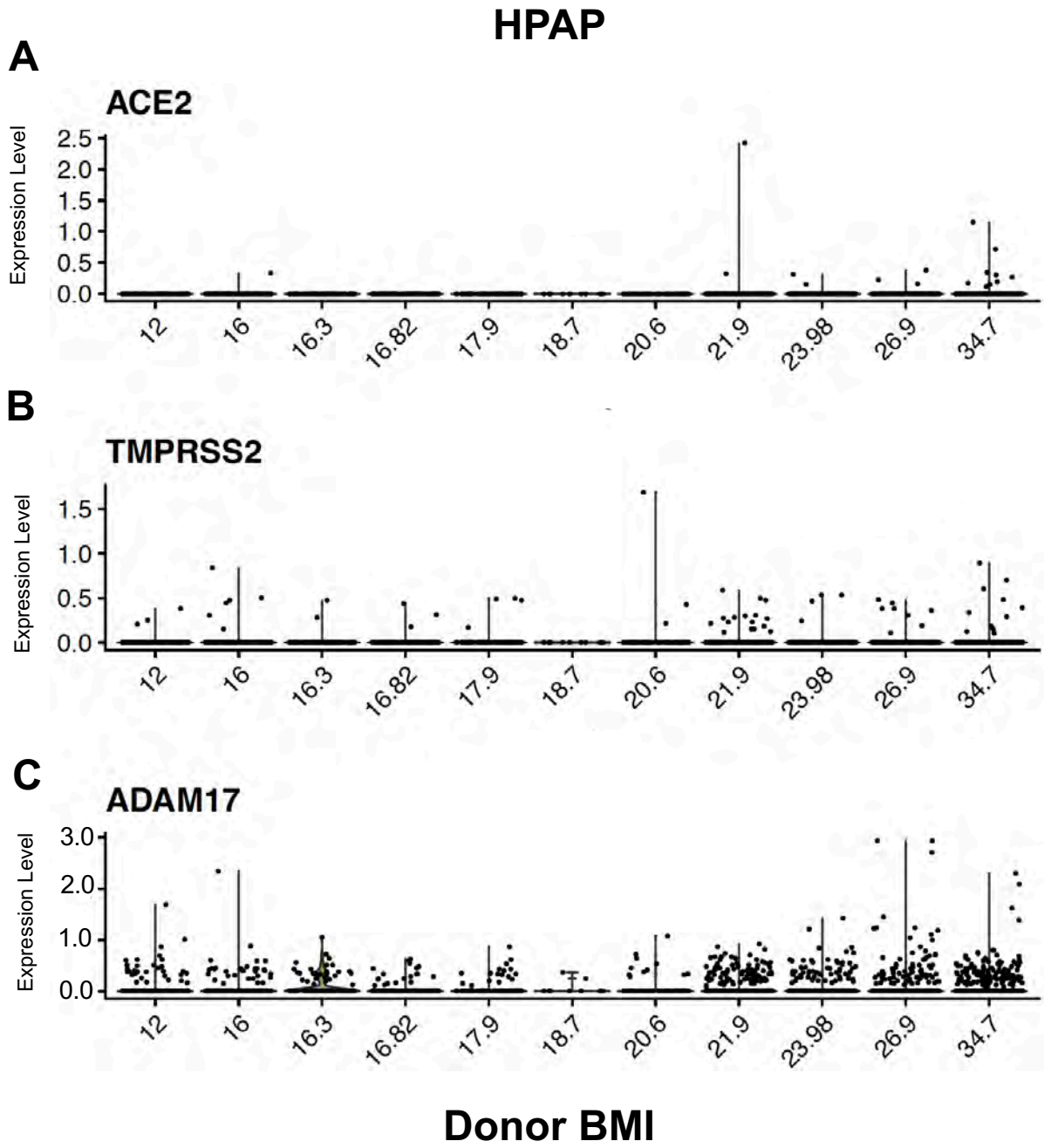
HPAP
A
ACE2
Expression Level
2.5
2.0
1.5
1.0
0.5
0.0
12
16
16.3
16.82
17.9
18.7
20.6
21.9
23.98
26.9
34.7
B
TMPRSS2
Expression Level
1.5
1.0
0.5
0.0
12
16
16.3
16.82
17.9
18.7
20.6
21.9
23.98
26.9
34.7
C
ADAM17
Expression Level
3.0
2.0
1.0
0.0
12
16
16.3
16.82
17.9
18.7
20.6
21.9
23.98
26.9
34.7
Donor BMI

Figure S2

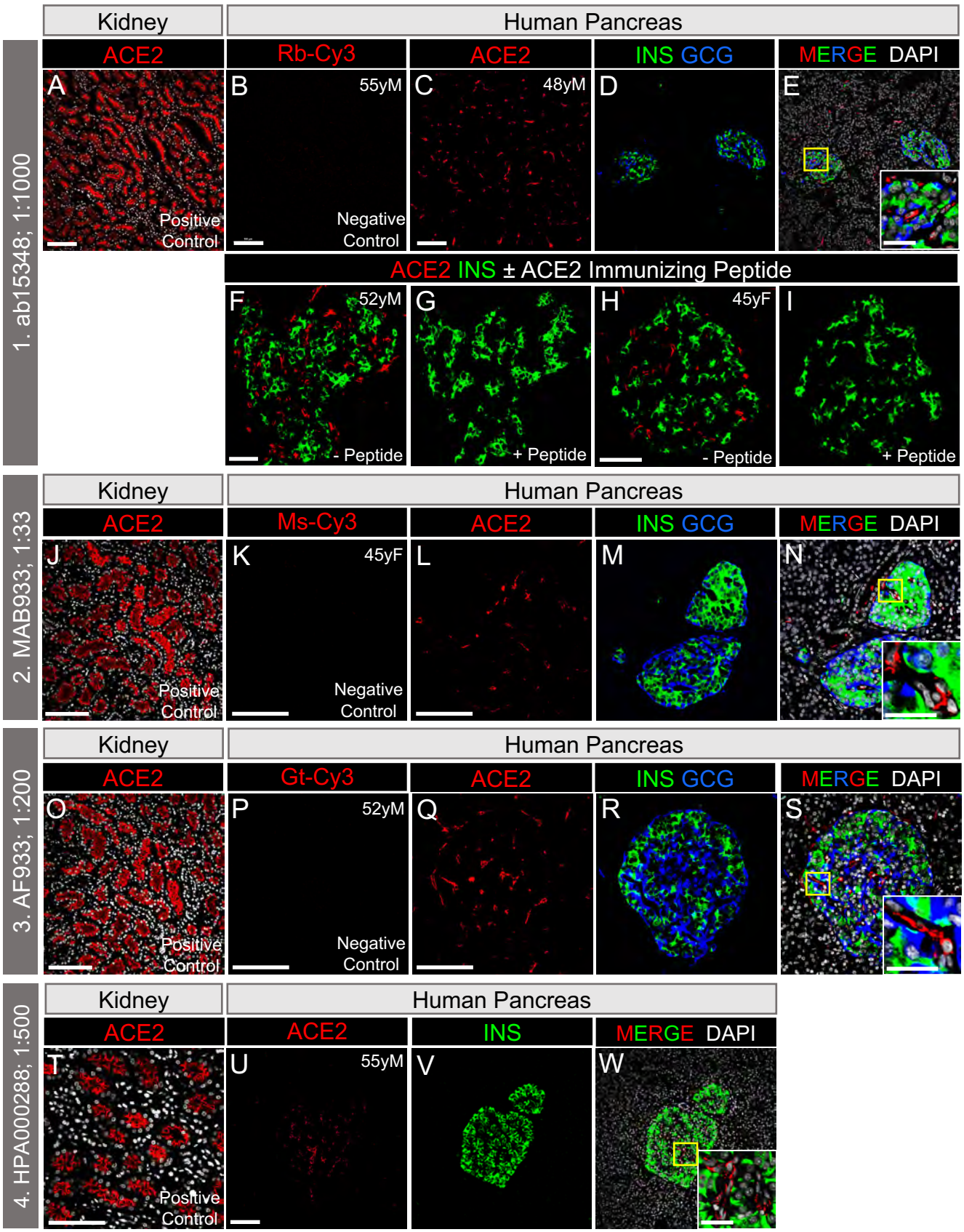
1. ab15348; 1:1000
Kidney
Human Pancreas
ACE2
Rb-Cy3
ACE2
INS GCG
MERGE DAPI
A
Positive Control
B
55yM
Negative Control
C
48yM
D
E
ACE2 INS ± ACE2 Immunizing Peptide
F
52yM
- Peptide
G
+ Peptide
H
45yF
- Peptide
I
+ Peptide
2. MAB933; 1:33
Kidney
Human Pancreas
ACE2
Ms-Cy3
ACE2
INS GCG
MERGE DAPI
J
Positive Control
K
45yF
Negative Control
L
M
N
3. AF933; 1:200
Kidney
Human Pancreas
ACE2
Gt-Cy3
ACE2
INS GCG
MERGE DAPI
O
Positive Control
P
52yM
Negative Control
Q
R
S
4. HPA000288; 1:500
Kidney
Human Pancreas
ACE2
ACE2
INS
MERGE DAPI
T
Positive Control
U
55yM
V
W

Figure S3

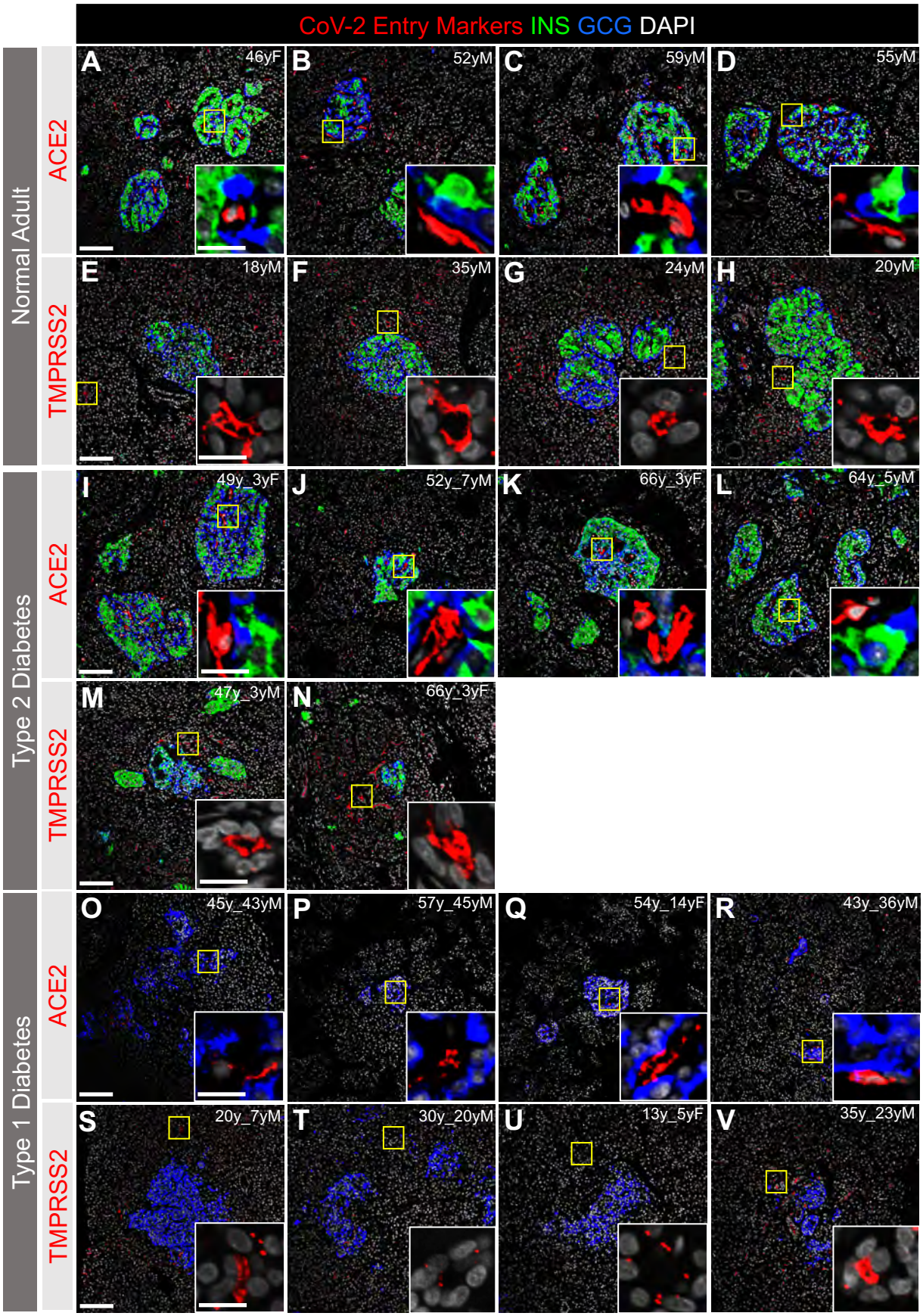
CoV-2 Entry Markers INS GCG DAPI
Normal Adult
ACE2
TMPRSS2
A 46yF
B 52yM
C 59yM
D 55yM
E 18yM
F 35yM
G 24yM
H 20yM
Type 2 Diabetes
I 49y_3yF
J 52y_7yM
K 66y_3yF
L 64y_5yM
M 47y_3yM
N 66y_3yF
Type 1 Diabetes
O 45y_43yM
P 57y_45yM
Q 54y_14yF
R 43y_36yM
S 20y_7yM
T 30y_20yM
U 13y_5yF
V 35y_23yM

Figure S4

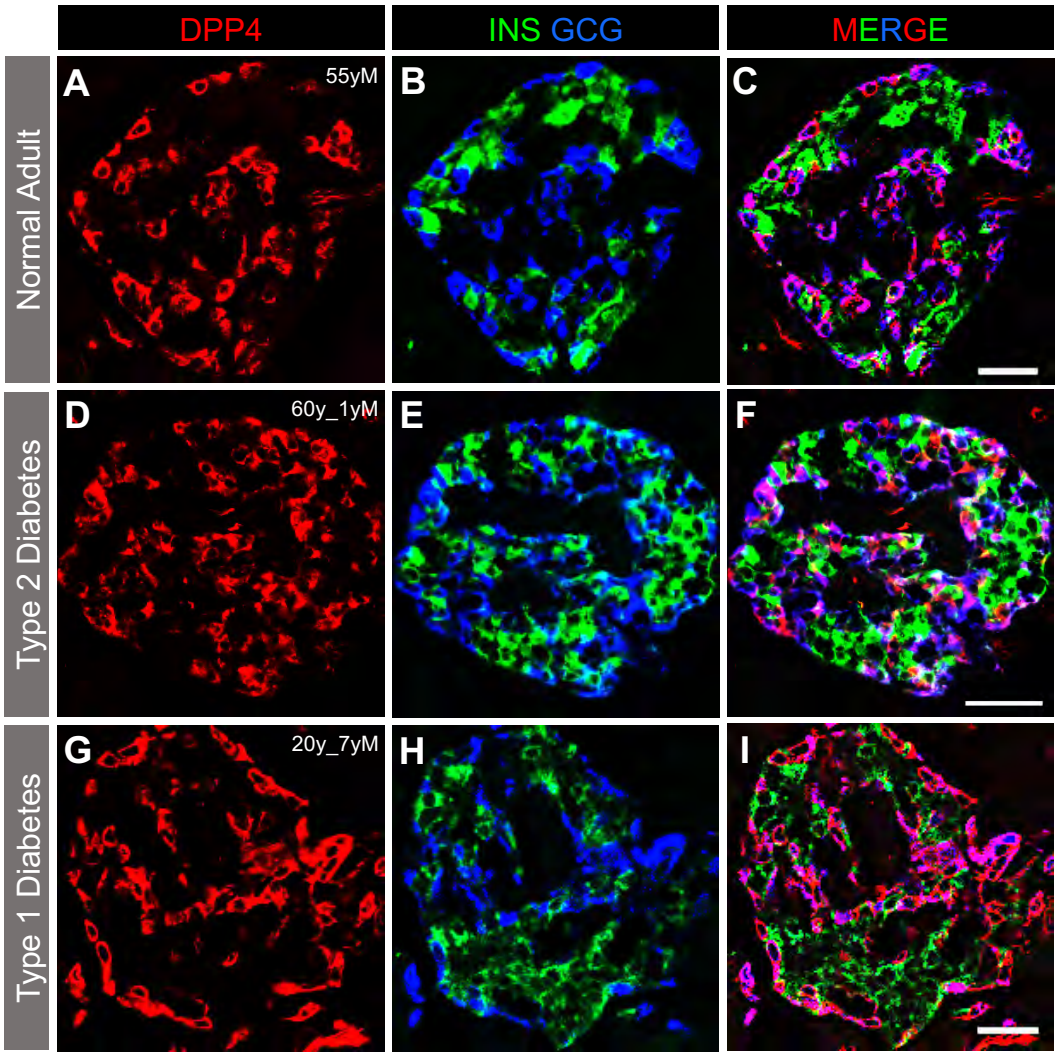
DPP4
INS GCG
MERGE
Normal Adult
Type 2 Diabetes
Type 1 Diabetes
A
55yM
B
C
D
60y_1yM
E
F
G
20y_7yM
H
I

J

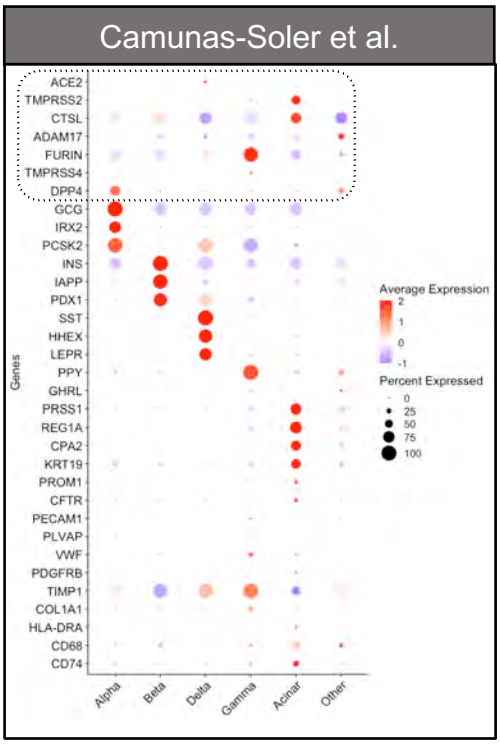
Camunas-Soler et al.
ACE2
TMPRSS2
CTSL
ADAM17
FURIN
TMPRSS4
DPP4
GCG
IRX2
PCSK2
INS
IAPP
PDX1
SST
HHEX
LEPR
PPY
GHRL
PRSS1
REG1A
CPA2
KRT19
PROM1
CFTR
PECAM1
PLVAP
VWF
PDGFRB
TIMP1
COL1A1
HLA-DRA
CD68
CD74
Genes
Alpha
Beta
Delta
Gamma
Acinar
Other
Average Expression
2
1
0
-1
Percent Expressed
0
25
50
75
100

Figure S5

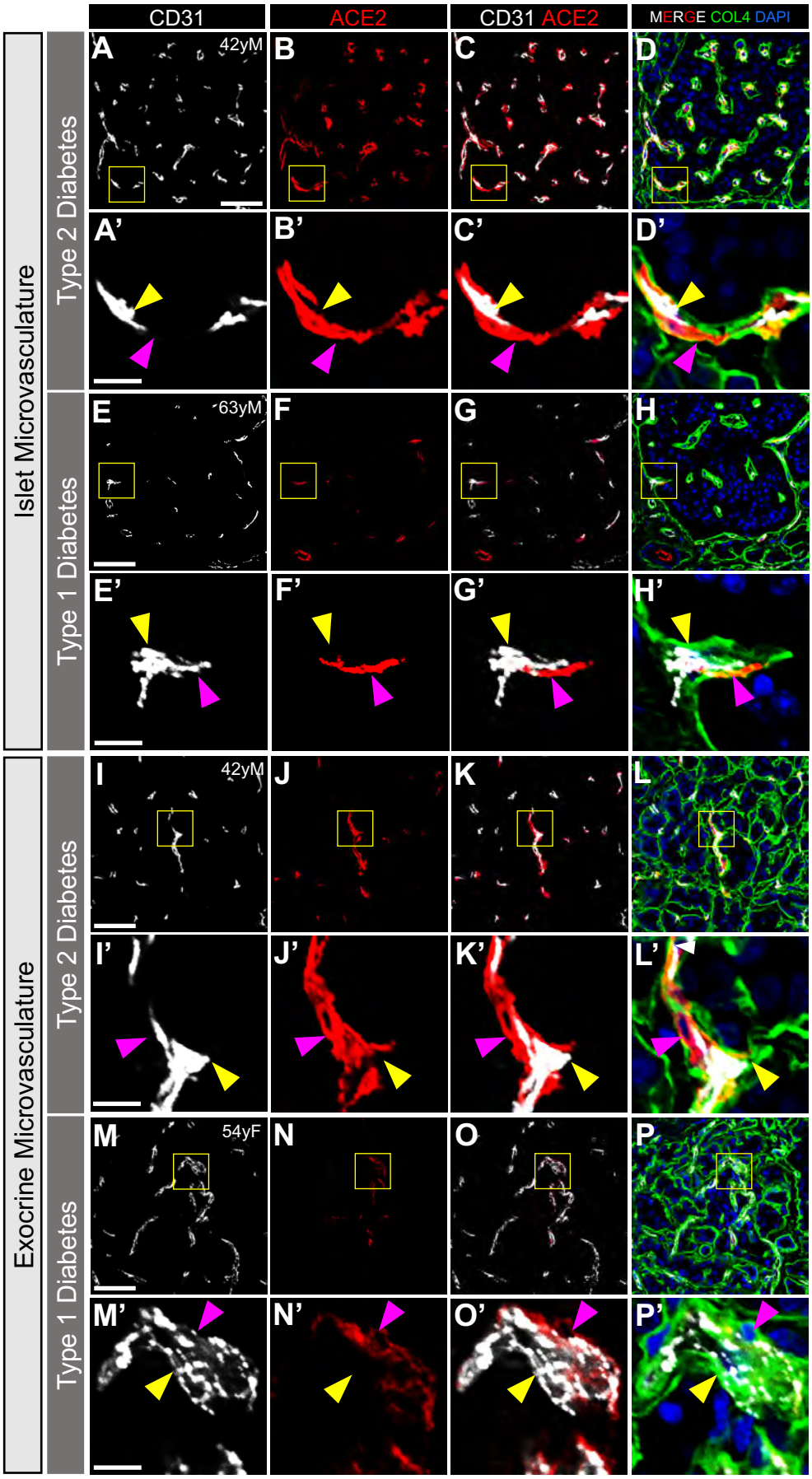
CD31
ACE2
CD31 ACE2
MERGE COL4 DAPI
Islet Microvasculature
Exocrine Microvasculature
Type 2 Diabetes
Type 1 Diabetes
Type 2 Diabetes
Type 1 Diabetes
A
42yM
B
C
D
A'
B'
C'
D'
E
63yM
F
G
H
E'
F'
G'
H'
I
42yM
J
K
L
I'
J'
K'
L'
M
54yF
N
O
P
M'
N'
O'
P'

KEY RESOURCES TABLE

REAGENT or RESOURCE	SOURCE	IDENTIFIER
Antibodies		
Mouse anti-Cytokeratin 19 (1:1000)	Abcam	Cat# ab194399
Rabbit anti-TMPRSS2 (1:400)	Sigma	Cat# HPA035787, RRID:AB_2674782
Mouse anti-Glucagon (1:500-1:1000)	Abcam	Cat# ab10988, RRID:AB_297642
Guinea pig anti-Glucagon (1:500)	LSBio	Cat# LS-C202759-50
Rat anti-C-peptide (1:1000)	DSHB	Cat# GN-ID4, RRID:AB_2255626
Guinea pig anti-Insulin (1:500-1:1000)	Dako	Cat# A0564, RRID:AB_2617169
Rabbit anti-ACE2 (1:500)	Atlas Antibodies	Cat# HPA000288, RRID:AB_1078160
Rabbit anti-ACE2 (1:1000)	Abcam	Cat# ab15348, RRID:AB_301861
Goat anti-ACE2 (1:200, Figure S1,3A-E; 1:400, Figure 4)	R&D	Cat# AF933, RRID:AB_355722
Mouse anti-ACE2 (1:33)	R&D	Cat# MAB933, RRID:AB_2223153
Mouse anti-CD31 (1:50)	BD Biosciences	Cat# 550389, RRID:AB_2252087
Goat anti-collagen IV alpha 1 (1:500)	Novus	Cat# NBP1-26549, RRID:AB_1853202
Goat anti-DPP4 (1:200)	R&D	Cat# AF1180, RRID:AB_354651
Mouse anti-NG2 [647] (1:50)	R&D	Cat# FAB2585R;
Goat anti-PDGFRβ (1:100)	R&D	Cat# AF385, RRID:AB_355339
Donkey anti-mouse-Cy2 (1:500)	Jackson ImmunoResearch	Cat# 715-225-150, RRID:AB_2340826
Donkey anti-mouse-Cy3 (1:500)	Jackson ImmunoResearch	Cat# 715-165-150, RRID:AB_2340813
Donkey anti-mouse-Cy5 (1:250 – 1:500)	Jackson ImmunoResearch	Cat# 715-175-151, RRID:AB_2340820
Donkey anti-rabbit-Cy3 (1:500)	Jackson ImmunoResearch	Cat# 711-165-152, RRID:AB_2307443
Donkey anti-rat-Cy2 (1:500)	Jackson ImmunoResearch	Cat# 712-225-153, RRID:AB_2340674
Donkey anti-guinea pig-Cy2 (1:500)	Jackson ImmunoResearch	Cat# 706-225-148, RRID:AB_2340467
Donkey anti-goat-Cy2 (1:500)	Jackson ImmunoResearch	Cat# 705-225-147, RRID:AB_2307341
Donkey anti-goat-Cy3 (1:500)	Jackson ImmunoResearch	Cat# 705-165-147, RRID:AB_2307351
Donkey anti-guinea pig-Cy5 (1:250-1:500)	Jackson ImmunoResearch	Cat# 706-175-148, RRID:AB_2340462
Normal Donkey Serum	Jackson ImmunoResearch	Cat# 017-000-121, RRID: AB_2337258
Bacterial and Virus Strains		
n/a		
Biological Samples		
Human pancreatic islets	Integrated Islet Distribution Program (IIDP)	http://iidp.coh.org, RRID: SCR_014387
Human pancreatic tissue	International Institute for the Advancement of Medicine (IIAM)	http://www.iiam.org, RRID: SCR_016172

Human pancreatic tissue	National Disease Research Interchange (NDRI)	http://ndriresource.org, RRID: SCR_000550
Chemicals, Peptides, and Recombinant Proteins		
Propidium Iodide	BD Biosciences	Cat# 556463
Antigen Unmasking Solution, Citrate-Based	Vector Laboratories	Cat# H-3300-250
1X PBS	Corning	Cat# 46-013-CM
Triton X-100	USB	Cat# 22686
BSA	Sigma	Cat# A6003-25G
Human ACE2 Peptide	Abcam	Cat# ab15352
Critical Commercial Assays		
RNAqueous-Micro Kit	Fisher Scientific (Invitrogen)	Cat# AM1931
High Capacity cDNA Reverse Transcription Kit	Fisher Scientific (Invitrogen)	Cat# 4368814
Deposited Data		
RNA-seq data for FACS purified human alpha and beta cells (Blodgett et al., 2015)	NCBI Gene Expression Omnibus	GEO: GSE67543
RNA-seq data for FACS purified human alpha and beta cells (Arda et al., 2016)	NCBI Gene Expression Omnibus	GEO: GSE57973
Single-cell RNA-seq data for human islets (Baron et al., 2016)	NCBI Gene Expression Omnibus	GEO: GSE84133
Single-cell RNA-seq data for human islets (Camunas-Soler et al., 2020)	NCBI Gene Expression Omnibus	GEO: GSE124742
Single-cell RNA-seq data for human islets (Segerstolpe et al., 2016)	ArrayExpress	E-MTAB-5061
Single-cell RNA-seq data for human islets (Human Pancreas Analysis Program [HPAP])	HPAP Database	https://hpap.pmacs.upenn.edu RRID:SCR_014393
Experimental Models: Cell Lines		
n/a		
Experimental Models: Organisms/Strains		
n/a		
Recombinant DNA		
n/a		
Software and Algorithms		
FV31S-SW Viewer 2.4.1.198	Olympus	https://www.olympus-lifescience.com/en/support/downloads/
Seurat 3.1 R package	(Butler et al., 2018) (Stuart et al., 2019)	N/A
Prism for macOS v.8.4.3	Graphpad Software	http://www.graphpad.com, RRID: SCR_002798
JACoP: Just Another Co-localization Plugin	ImageJ	https://imagej.nih.gov/ij/plugins/track/jacop2.html